NONLINEAR CONTROL OF ACTIVE PNEUMATIC SUSPENSIONS

by

ROBERTO BARLETTA

Ingeniero Mecanico, Universidad
Simon Bolivar, Venezuela
(1982)

SUBMITTED TO THE DEPARTMENT OF
MECHANICAL ENGINEERING IN PARTIAL
FULFILLMENT OF THE REQUIREMENTS
FOR THE DEGREE OF

MASTER OF SCIENCE IN
MECHANICAL ENGINEERING

at the

MASSACHUSETTS INSTITUTE OF TECHNOLOGY

May 1984

Signature of Author 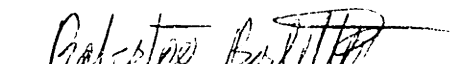
Department of Mechanical Engineering
May, 1984

Certified by 
J. Karl Hedrick
Thesis Supervisor

Accepted by 
Warren M. Rohsenow
Chairman, Departmental Graduate Committee

NONLINEAR CONTROL OF ACTIVE PNEUMATIC SUSPENSIONS

by

ROBERTO BARLETTA

Submitted to the Department of Mechanical Engineering on May 10, 1984, in partial fulfillment of the requirements for the degree of Master of Science in Mechanical Engineering.

ABSTRACT

The effectiveness of using a simple nonlinear on-off controller with lead compensation and hysteresis as a means of controlling a pneumatic active suspension system is evaluated. The ride quality improvement that can be achieved using this nonlinear active pneumatic suspension system in parallel with passive springs and dampers is investigated. A one degree of freedom model is used to simulate the lateral dynamics of a conventional passenger rail vehicle to pseudo-random disturbances entering from the truck.

A set of experiments is used to evaluate the accuracy of the analytical model. The performance of the system for different actuators and valves is evaluated using computer simulation. The feasibility of using semi-active suspension systems as a means of improving ride quality performance while reducing the system power consumption is considered.

It is found by means of computer simulation that using 4 inch bore pneumatic cylinders as actuators and solenoid valves with a nominal air flow capability of 50 scfm, a 49% reduction in the r.m.s. carbody lateral acceleration, and a 22% reduction in the r.m.s. lateral suspension stroke can be achieved while requiring 9.3-13.7 horsepower/car.

It is concluded that the simplicity, low cost and high reliability of this nonlinear active pneumatic suspension system, make it a promising method to improve the ride quality performance of rail vehicles.

Thesis Supervisor: Dr. J. Karl Hedrick.
Title: Professor of Mechanical Engineering.

ACKNOWLEDGEMENTS

The author expresses his appreciation to Professor J. Karl Hedrick. His invaluable guidance and advice were vital to this effort.

I would like to thank my friend Gustavo Weber for his countless technical contributions and his continuous support and encouragement.

The author wishes to express his appreciation to Neal Dahlem for his interest and constructive comments, and to Ricardo Morchio for his friendship and helpful advice.

I would like to express my gratitude to CEPET, the Venezuelan Petroleum and Petrochemical Formation and Training Center, that gave me the financial support to make possible this study.

Lastly, and most important, I thank my parents and brother for their unfailing love and moral support.

TABLE OF CONTENTS

LIST OF FIGURES

LIST OF TABLES

Chapter 1

INTRODUCTION

Although many vibration problems are solved in an inexpensive, reliable, and satisfactory way with passive devices, it is clear that there are distinct performance limitations when only passive elements are used. In the past, many attempts were made to improve vibration control devices by providing some adjustable parameters, such as spring and damper coefficients, which could be varied to suit changing exitation or response characteristics. Such variable parameter systems can have better vibration isolation and represent a simple form of control loop used to improve performance.

As high-performance servomechanisms were improved and simulation methods for automatic control systems were developed, the use of such "active" parameters became more common. Although the active vibration control systems give, in general, better performance than the best possible passive system, economical limitations and the fact that they are less reliable than passive systems, have restricted their use to cases in which very high performance is required.

The objective of this research is to evaluate the performance of an active pneumatic suspension device which using a simple control law would be able to improve, in an economical and reliable way, the ride quality performance of rail vehicles.

1.1 BACKGROUND

In a traditional passenger rail vehicle, the dynamics of motion can be subdivided into two decoupled sets of rigid body modes [1] consisting of lateral, yaw and roll modes in the lateral dynamics and longitudinal, heave and pitch modes in the vertical dynamics (Fig 1.1.1). For simplicity, it is convenient to analyze and design the suspension of rail vehicles as a decoupled set of lateral and vertical suspension elements.

The primary purpose of the lateral rail vehicle suspension elements are: to provide "tracking" of intentional inputs such as curves and switches, to isolate the truck and carbody from unintentional disturbances such as random track irregularities and rail joints, and to damp all modes, specially the kinematic or the "hunting" mode. To perform these tasks, the lateral suspension of rail vehicles is usually divided into two sets of independent suspensions (Fig.

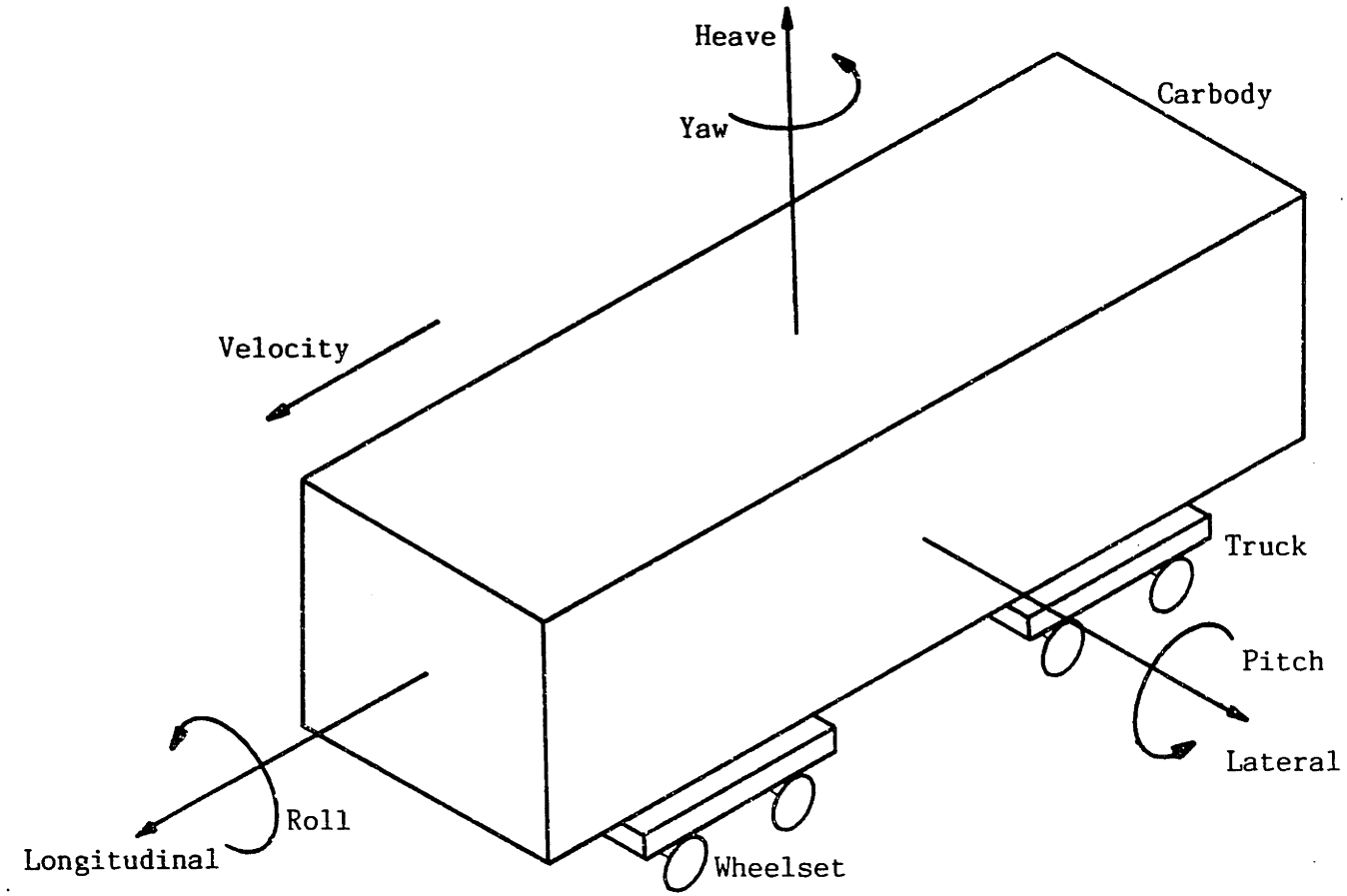

FIGURE 1.1.1 DEFINITION OF DIRECTIONAL TERMINOLOGY.

1.1.2). The primary suspension, placed between the wheelset and the truck, and the secondary suspension that connects each of the two trucks to the carbody.

The primary suspension is largely determined by the lateral stability/curving trade off [1], while the secondary suspension is largely determined by the ride quality/suspension stroke trade off [2].

Generally, a soft secondary suspension attenuates carbody accelerations more than a stiff suspension, at the expense of a larger suspension stroke. The lateral secondary suspension, is usually limited in its travel for such reasons as avoiding sideswiping tunnels or other trains and limiting carbody excursions during curving or wind gusts. When the carbody moves laterally more than a prefixed value, relative to the truck, it encounters bumpstops that increase the lateral stiffness a significant amount, greatly reducing further travel of the carbody. This, of course, increases lateral accelerations deteriorating the ride quality.

It has been shown that with well-laid, well-maintained tracks, lateral carbody accelerations can be greatly reduced, even at high operating speeds [3,4]. However, in many cases it is more economically feasible to consider innovative suspension designs, as a practical solution to reduce lateral accelerations. Ride quality is primarily determined by lateral accelerations. At moderate exposure levels, these

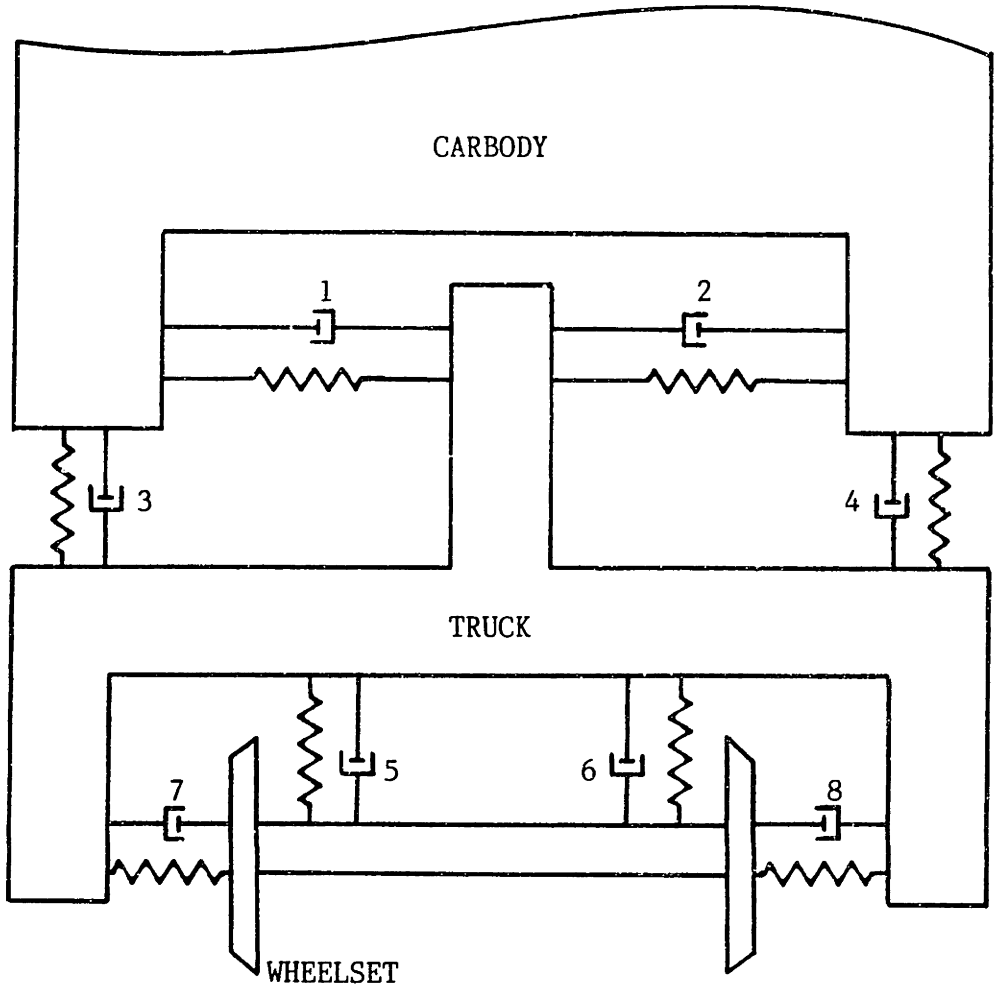

1,2 Lateral secondary suspension

3,4 Vertical secondary suspension

5,6 Vertical primary suspension

7,8 Lateral primary suspension

FIGURE 1.1.2 SCHEMATIC OF VEHICLE PRIMARY AND SECONDARY SUSPENSIONS.

accelerations can cause reduced comfort, fatigue at higher exposure levels, and eventually dizziness and motion sickness at extreme levels. Figure 1.1.3 shows the human exposure limits to lateral accelerations as established by the International Organization For Standarization I.S.O. [5]. The exposure limit is a function of the frequency and duration of the accelerations. Special care should be taken for low frequency accelerations in order to improve ride quality.

Much research has been done in order to improve "lateral ride quality" by means of using passive suspension elements [6]. Several types of nonlinear springs and dampers as well as different configurations of the "suspension elements" have been studied. However, it has been shown [7] that only moderate improvements can be achived by passive means.

Studies done at M.I.T. [8] have shown that the addition of active elements to a passive suspension can improve passenger comfort beyond the limits possible when only passive elements are used.

1.2 ACTIVE SUSPENSIONS

Passive suspensions are limited by the restriction that forces can only be created from local, relative motion

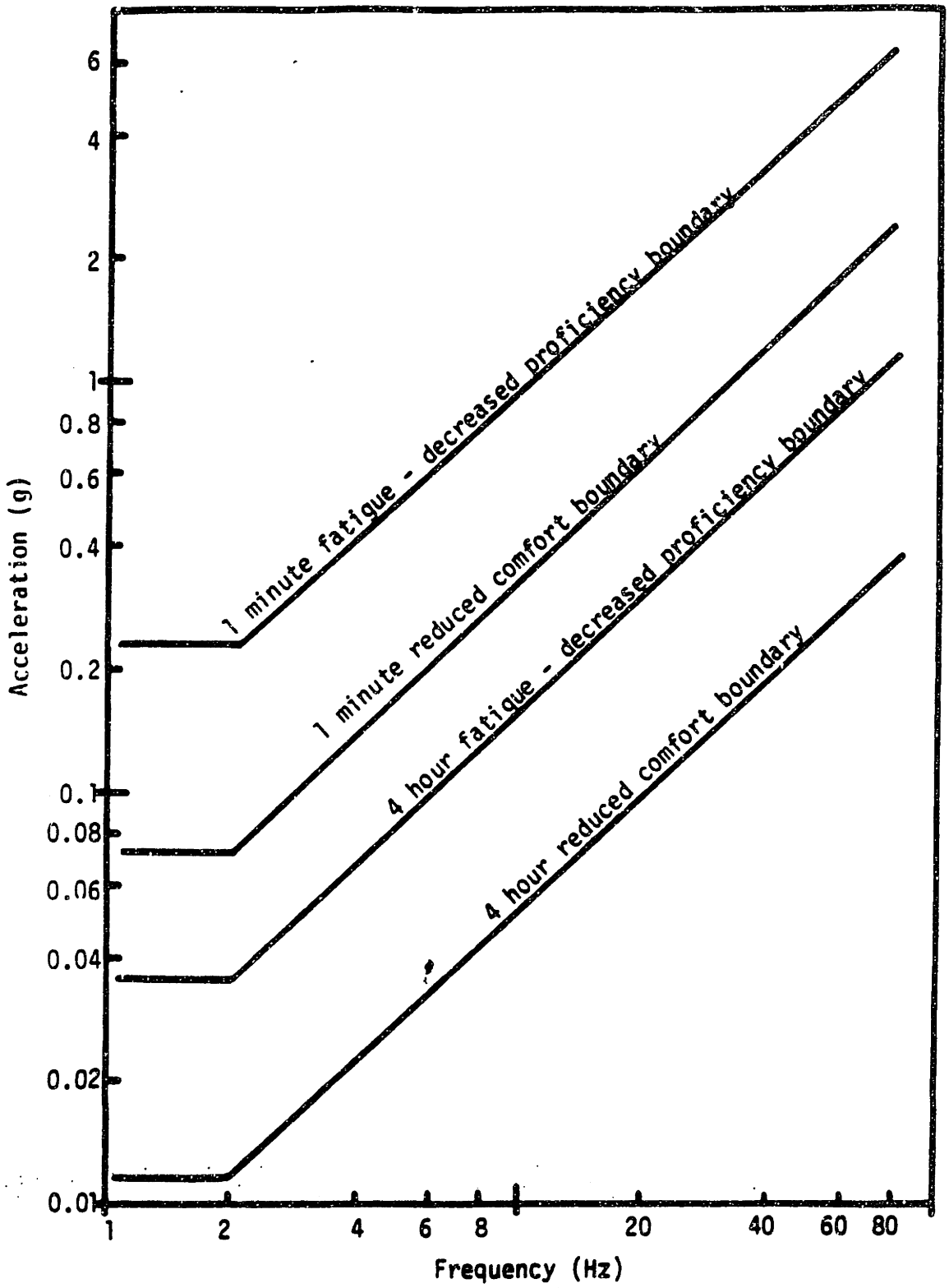

FIGURE 1.1.3 TRANSVERSE ACCELERATION LIMITS AS A FUNCTION OF FREQUENCY AND EXPOSURE TIME.

and energy can only be dissipated or stored and used later. Active suspensions, however, do not have either of these restrictions. Forces created by actuators can be related to any state or combination of states one is able to measure. External power is used to supply the energy required by these actuators.

Actuator forces in semi-active and semi-passive suspensions, can also be related to any given state. Since external power is only used for measuring and conditioning the sensor signals and not for applying energy to the system, much less power is required. Therefore, semi-active and semi-passive suspensions are more economical, but the improvement in performance that can be achived is less significant than using fully active suspensions [9].

1.3 PREVIOUS WORK IN ACTIVE SUSPENSIONS AT M.I.T.

Using a 15 degree of freedom model of an Amcoach Amtrak train, Celniker [10] showed that with a "local ride control" which applied the control force between the carbody and the truck, the r.m.s. lateral acceleration can be reduced by 67% and the secondary r.m.s. suspension stroke can be reduced by 17%. His simulation assumed ideal actuators and a control law given by:

$$Fd = - K1 \ddot{Y}c - K2 \dot{Y}c \qquad (1.3.1)$$

where: Fd is the desired actuator force; $\ddot{Y}c$ is the carbody absolute acceleration; $\dot{Y}c$ is the carbody absolute velocity, and K1 and K2 are the acceleration and velocity feedback gains respectively.

Hedrick and others [11] measured lateral accelerations of an Amtrak passenger-coach carbody traveling on the Northeast corridor (New York City to Washington D.C.) to determinate the frequency and magnitude of the accelerations. The results showed that most of the accelerations were in the 0.5-2 Hz frequency region.

Buzan [12] used a one degree of freedom model, to simulate half of the vehicle dynamics (half of the carbody and one truck), to a random position disturbance entering from the truck. He used an actuator having a first order lag in parallel with the passive spring and damper, and introduced to the Celniker's control law a force feedback gain "Kf" which multiplied the difference between the desired force, Fd, and the actuator force, Fa (Fig. 1.3.1).

His simulation showed that an actuator with a 3 Hz bandwidth could be successfully used to attenuate carbody accelerations. He selected Firestone 225 airsprings as actuators and modeled the filling and exhausting of these actuators using a pneumatic proportional valve. He showed that the r.m.s. acceleration could be reduced 40% and the

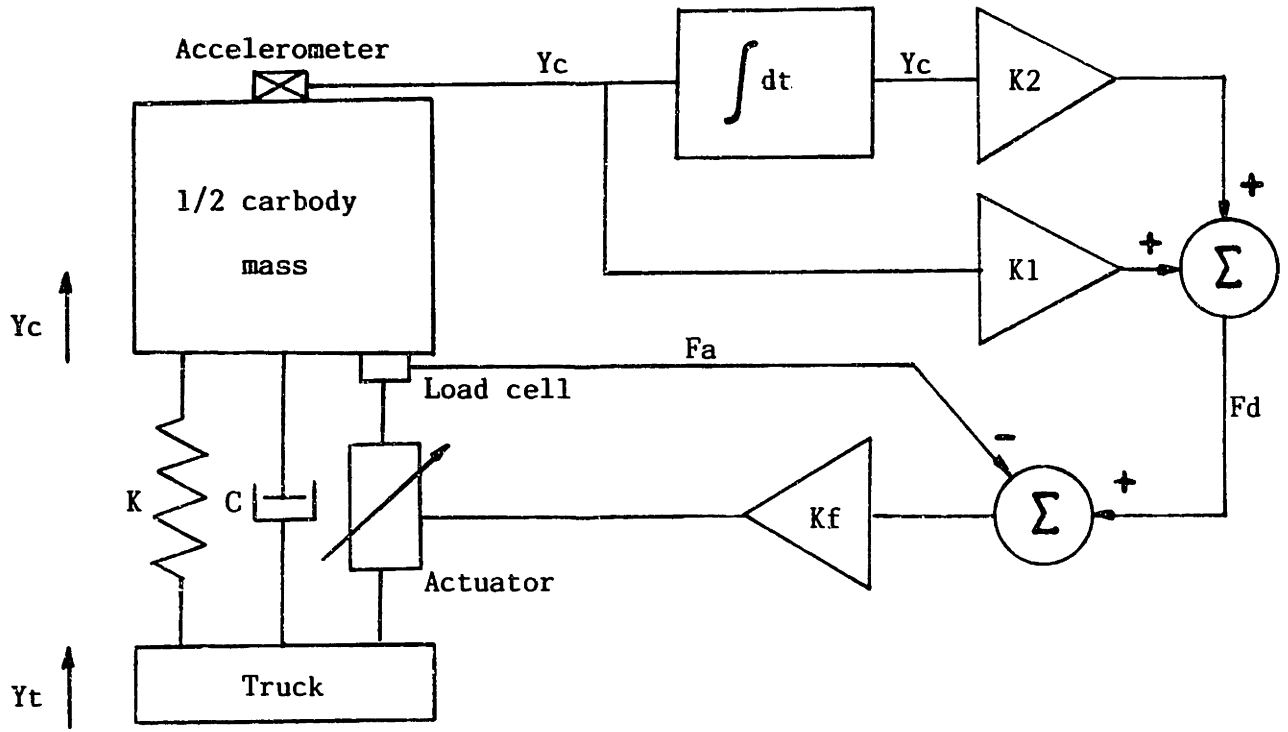

FIGURE 1.3.1 SCHEMATIC OF ONE HALF PASSENGER RAIL VEHICLE MODEL WITH "LOCAL RIDE CONTROLLER".

r.m.s. stroke could be reduced 12% with a power consumption of 27-38 horsepower/car.

To reduce the power consumption, Cho [13] studied the effectiveness of different actuators and proportional valves. He simulated a typical disturbance input and showed that, with a pneumatic proportional valve with a peak flow capability of 40 scfm and using a 4 inch bore pneumatic cylinder as an actuator, the lateral r.m.s. acceleration of the passenger compartment could be reduced by 46% with a power consumption of 5.4 to 7.5 horsepower/car. To increase the reliability of the system and to reduce installation costs, De Los Reyes [14] studied the feasibility of using pulse width modulation as a method of controlling a solenoid valve in a pneumatic active suspension. He showed that control via pulse width modulation did not yield satisfactory performance because commercially available solenoid valves do not have a high enough bandwidth.

1.4 SCOPE OF THIS THESIS

The purpose of this thesis is to show that with a nonlinear on-off controller, a solenoid pneumatic valve can be driven to produce good isolation performance while using a "relatively" low power consumption in a pneumatic active suspension system.

Towards this end, a set of analytical models as well as some experimental tests were implemented. Chapter two, describes the specifications and restrictions of the control problem. It also gives some motivation for the implementation of the control used, and a description of the simulation techniques utilized. Chapter three, contains the electrical design of the controller, a description of the experimental set up and the evaluation of the digital model used throughout this thesis. The performance of the system when using a 1 D.O.F. model as well as some parametric studies on the effect of changing the different parameters involved are discussed in chapter four. The effectiveness of using semi-active suspensions in order to reduce power consumption is discussed in chapter five. In chapter six, the conclusions reached and the recommendations for future work are presented. FORTRAN codes of the programs used for the simulations are presented in the appendices.

Chapter 2

BANG-BANG CONTROL OF ACTIVE PNEUMATIC SUSPENSIONS

2.1 INTRODUCTION

The success of any active suspension system applied to rail vehicles depends to a large degree on its reliability, simplicity and low installation, operation and maintenance costs. References [6], [12] and [13] show that using a proportional "local ride controller" the ride quality/stroke trade-off can be successfully resolved. However, this controller requires the utilization of a proportional valve. When air is used as a working fluid, the power consumption and therefore the flow required, are considerable increased with respect to those needed by a hydraulic system. In this case, proportional valves capable of handling the required air flow are difficult to find, and they are expensive.

To overcome these economical limitations, De Los Reyes [14], studied the feasibility of using a pulse width modulated

controller to drive a pneumatic solenoid on-off valve. However, solenoid valves commercial available, although very inexpensive, are in general "slow", and have significant time delays in the opening and closing process. For pulse width modulation to work, a solenoid valve of at least 20 hz is required [15]. Although such a valve can be constructed, it would be expensive and probably a pneumatic proportional valve would be preferred.

A bang-bang control law was proposed as a simple way of driving a solenoid valve, while overcoming the above limitations. The idea behind this controller, as well as the considerations required for its digital simulation, are presented in this chapter.

2.2 DESCRIPTION OF THE PROBLEM

As stated before, the dynamics of motion of a passenger rail vehicle can be subdivided into a decoupled set of vertical and lateral body modes. Although the ride quality is related to the lateral and vertical acceleration among other factors, the stroke limitations in the vertical direction are less severe, and passive suspension elements can be chosen to give the desired performance.

In the lateral direction, however, the constraints are

more severe. For a typical Amtrak passenger car, the maximum allowable peak to peak secondary stroke is limited to 1.5 inches. This greatly reduces the amount of isolation that can be achived by passive means. Thus, active suspensions give an alternative to further reduce lateral vibration of the passenger car.

It is possible to modify the primary lateral suspension to reduce lateral accelerations. However, practical considerations suggest that the implementation of a new primary suspension, either active or passive, is economically impractical if the existing trucks are to be used. This is because of the limited space available, and the severe working conditions under which these primary suspensions must operate.

To simplify the active suspension design, a one degree of freedom model was chosen to simulate the carbody lateral dynamics (Fig. 2.2.1). For this model, it was assumed that one half of the mass of the carbody could be considered as a lumped mass M, supported by a conventional spring K, and damper C, mounted in parallel and connected to the truck. The input of the system was then given by the displacement of the truck, Yt. Using the notation of Fig. 2.2.1 the equilibrium equation of the system is given by:

$$M\ddot{Y}c + C(\dot{Y}c-\dot{Y}t) + K(Yc-Yt) = 0. \qquad (2.2.1)$$

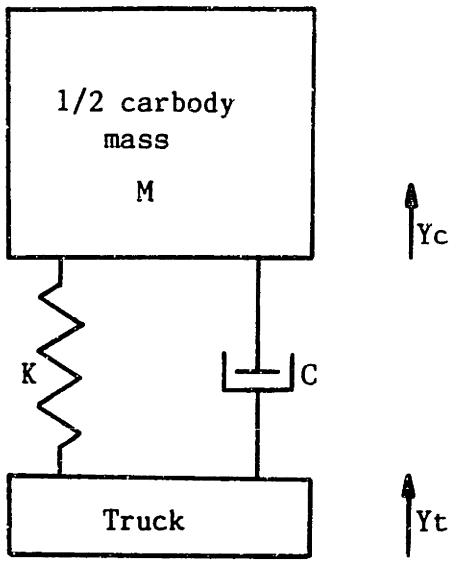

FIGURE 2.2.1 ONE DEGREE OF FREEDOM MODEL.

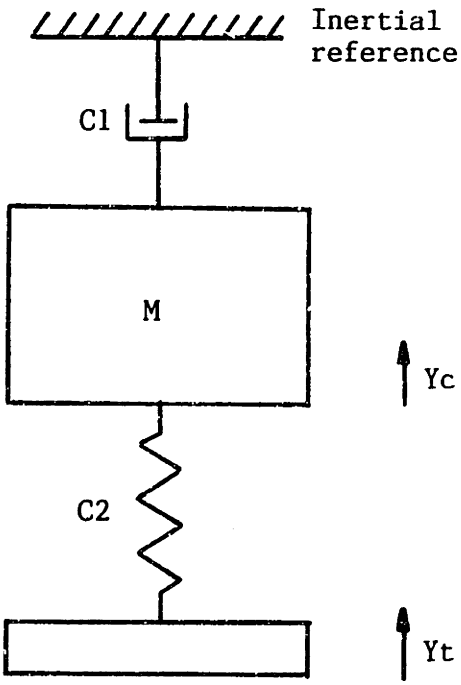

FIGURE 2.2.2 THE "SKYHOOK" DAMPER SYSTEM.

For this passive case, the force acting on the mass is given by:

$$Fr = - C(\dot{Y}c-\dot{Y}t) - K(Yc-Yt) \qquad (2.2.2)$$

If one assumes that this force is not held to the passive elements, but instead, that it can be generated as a function of the state variables of the system, i.e. the absolute carbody velocity $\dot{Y}c$, and the absolute carbody displacement Yc, a linear quadratic criteria can be used to find the optimal force that minimizes the square carbody velocity and the square system stroke. It can be shown, that for a random guideway input, the optimal force Fc is given by:

$$Fc = - C1\ \dot{Y}c - C2(Yc-Yt) \qquad (2.2.3)$$

where: C1 and C2 are constants that depend on the cost matrix chosen. It should be noticed that the carbody acceleration is a linear combination of the relative velocity and displacement of the carbody, and that by minimizing these variables we are also minimizing the absolute carbody acceleration.

The feedback law given by Eq. 2.2.3 can be realized by passive elements if a damper can be placed between the mass M, and some inertial reference (Fig. 2.2.2). This, of course, can not be done on rail vehicles, therefore some active component should be / introduced into the system to minimize acceleration.

In the train, the secondary suspension lateral stiffness is produced by the shear force of the secondary vertical suspension spring. A hydraulic damper connected between the carbody and the truck is responsable for the damping coefficient (Fig. 2.2.3). This configuration, makes it very costly to change the lateral secondary stiffness. To avoid an undamped system response in the case of active suspension failure, it is recommended to have some passive damping on the system even when the active controller is being used. For these reasons, it was decided that an actuator working in parallel with these two passive components should be used. The values of these and other parameters for an Amtrak passenger-coach used as example in this thesis, are listed in Table 2.1.

Hedrick and others [6] have shown that a control law of the form:

$$Fd = - K1 \ddot{Y}c - K2 \dot{Y}c \qquad (2.2.4)$$

where Fd is the force generated by the actuator, could be successfully used. This control law requires absolute velocity and acceleration feedback. Sensing the velocity is an impractical task, however, it has been shown [14] that by high passing the signal coming from an accelerometer, and integrating it, a good estimate of the absolute velocity of the carbody can be obtained. In this way, only an accelerometer is needed to implement control law 2.2.4.

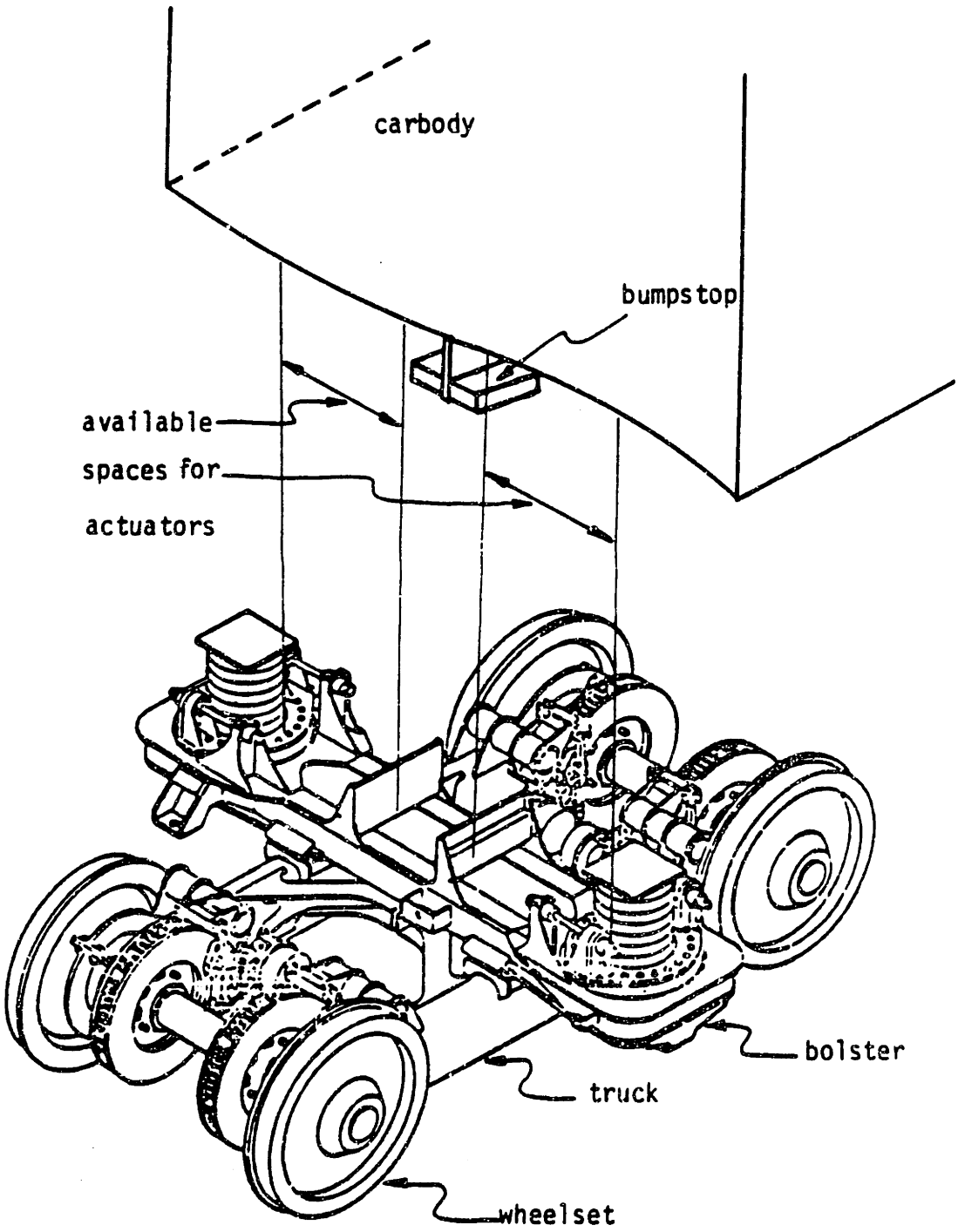

FIGURE 2.2.3 TRUCK CONFIGURATION.

TRUCK PARAMETERS		
1/2 of primary spring lateral spacing	1.9	ft
1/2 of wheelbase	4.25	ft
truck frame mass	212	slugs
CARBODY PARAMETERS		
1/2 of secondary spring lateral spacing	3.27	ft
1/2 of truck center pin spacing	30	ft
carbody mass	2405	slugs
PRIMARY SUSPENSION PARAMETERS		
primary lateral stiffness (4 per truck)	480000	lb/ft
primary longitudinal stiffness (4 per truck)	960000	lb/ft
primary lateral damping	2020	lb-sec/ft
primary longitudinal damping	2850	lb-sec/ft
SECONDARY SUSPENSION PARAMETERS		
secondary lateral stiffness (2 per truck)	24000	lb/ft
secondary vertical stiffness (2 per truck)	22200	lb/ft
secondary lateral damping (2 per truck)	1200	lb-sec/ft
secondary vertical damping (2 per truck)	2000	lb-sec/ft

Table 2.1.- BASELINE AMCOACH PARAMETERS [13]

The equilibrium equation of the system when an actuator is used is given by:

$$M\ddot{Y}c + C(\dot{Y}c-\dot{Y}t) + K(Yc-Yt) - Fd = 0 \qquad (2.2.5)$$

or using 2.2.4:

$$(M+K1)\ddot{Y}c + K2\ \dot{Y}c + C(\dot{Y}c-\dot{Y}t) + K(Yc-Yt) = 0 \qquad (2.2.6)$$

It can be seen from this equation, that the acceleration feedback gain K1, has the effect of "increasing" the mass of the system, therefore reducing the transmissibility. The velocity feedback gain K2, on the other hand, introduces a term in the equation that is equivalent to the one given by equation 2.2.3, i.e. it simulates the effect of a passive damper connected between the mass and some inertial reference.

This scheme of control, where the acceleration of the carbody above the truck is sensed and fed back to the actuators located between that truck and the carbody, is known as "local ride quality control".

Hydraulic proportional active suspensions using the control law given in 2.2.4 were shown to significantly reduce lateral acceleration with a relatively low power consumption (3 to 5 horsepower/car) [10]. However, since most of the train equipment is pneumatic powered, it was decided that the active suspension to be developed should also be pneumatic powered.

Pneumatic equipment maintenance is "cleaner", and the train company personnel have a considerable amount of experience in working with this kind of equipment. In addition, the train locomotive is already equiped with an air compressor that may be utilized to power the active suspension system without further equipment installation. Pneumatic actuators also are safer in the case of system failure since block-off of the actuators can rarely occur.

2.3 THE CONTROL LAW

To implement control law 2.2.4 using a pneumatic cylinder actuated by a solenoid servovalve, an on-off controller with lead compensation and hysteresis has been proposed (Fig 2.3.1)

In this controller, a reference or desired force is generated using equation 2.2.4. This desired force is then compared with the actual force in the actuator, sensed by means of a load cell, and the resultant error is passed through a lead compensator. When the "compensated error" Ec is bigger than a pre-set amount Fr, the input valve of the pneumatic cylinder opens, letting the air coming from the pressure supply go to the cylinder, thereby increasing the pressure and the force produced by the actuator. If the "compensated error" is less than a pre-set value -Fr, the

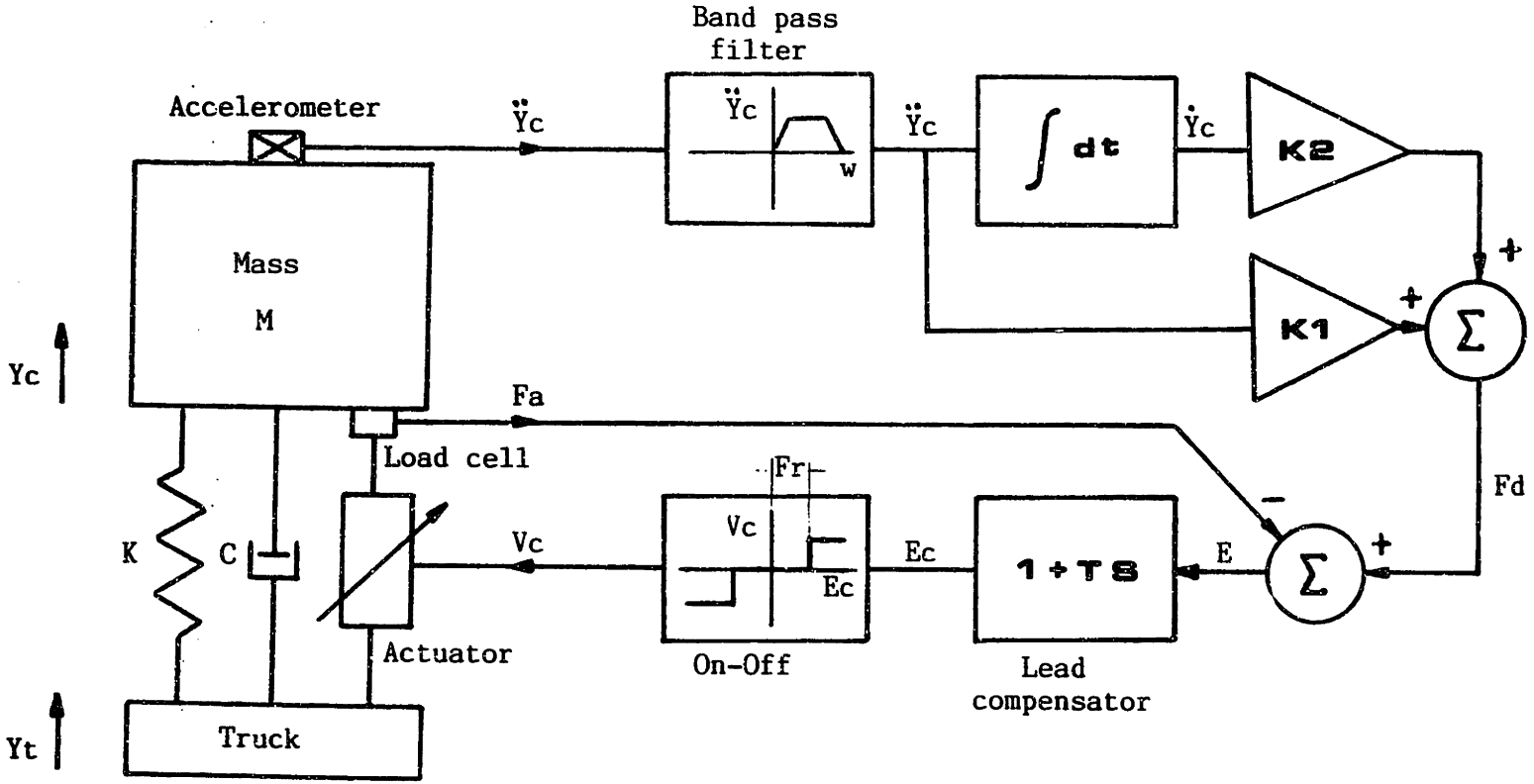

FIGURE 2.3.1 THE CONTROL LAW.

output valve of the pneumatic cylinder opens releasing the air of the cylinder into the atmosphere and reducing the force applied by the actuator. When the "compensated error" is less than Fr but bigger than -Fr both valves remain close and the amount of air in the cylinder remains constant.

In the real system implementation, two pneumatic cylinders per truck are required to generate positive and negative forces. Therefore four valves per truck are required. In this configuration, the input valve of one cylinder acts at the same time as the output valve of the other cylinder in such a way that when one cylinder is being filled up the other is being emptied.

The lead compensator was introduced in the control law because pneumatic solenoid valves have pure time delays in the opening and closing process. The lead compensator tends to decrease the effect of these delays in the response of the system. The lead compensation also reduces limited cycling in nonlinear systems. A low pass filter is required in order to implement the lead compensation since high frequency noise must be attenuated.

The band pass filter at the output of the accelerometer is used to attenuate this high frequency noise and to eliminate d.c. accelerations generated in curving or tilt of the accelerometer, since no response of the active system is desired in these cases. The band pass filter is

also required to obtain good estimates of the velocity in the integration process.

The dead zone of the on-off controller has been included to avoid oscillations in steady state. When the difference between the desired force Fd, and the actual actuator force Fa, is less than a certain amount, the closing time delay of the valve makes it impossible to compensate this error, driving the actuator force to a value which is either bigger or smaller than the desired one. This, produces oscillations that will not be attenuated in steady state. These oscillations can be avoid by choosing a convenient value for the dead zone Fe. The value of Fe depends primarily on the closing time delay, the valve area, the actuator diameter and the pressure supply. The choice of Fe for different values of these parameters is shown in chapter four.

2.4 DIGITAL SIMULATION OF NONLINEAR ACTIVE SUSPENSIONS

To evaluate the performance of pneumatic active suspensions when using the stated control law, a FORTRAN program was written (appendix 2). This program, runs with a fourth order Runge-Kutta routine that integrates the nonlinear equations that describe the system.

The model of each of the components of the active

suspension system used by this program, as well as the way the input disturbance was formulated is explained in this section.

2.4.1 Input Disturbance

To predict the performance of active suspensions, when applied to rail vehicles, Cho [13] developed an analytical model that simulates the truck displacement and velocity when traveling at constant speed in the Northeast corridor. In this model, nine sine waves ranging three octaves were summed to represent the truck displacements. The truck velocity was represented by the derivative of the truck displacements. A comparison between the simulated results and the experimental data [11,18], showed that the analytical formulated disturbance was a reasonably accurate description of the vehicle operating conditions.

Figure 2.4.1 shows the power spectral density of the carbody lateral acceleration when using the simulated disturbance. It can be seen, that for a passive suspended Amtrak passenger-coach, the lateral carbody acceleration is primarily a 0.5-2 hz phenomenon. These low frequency accelerations, are attributed to the secondary lateral suspension which has a natural frequency of about 1 hz.

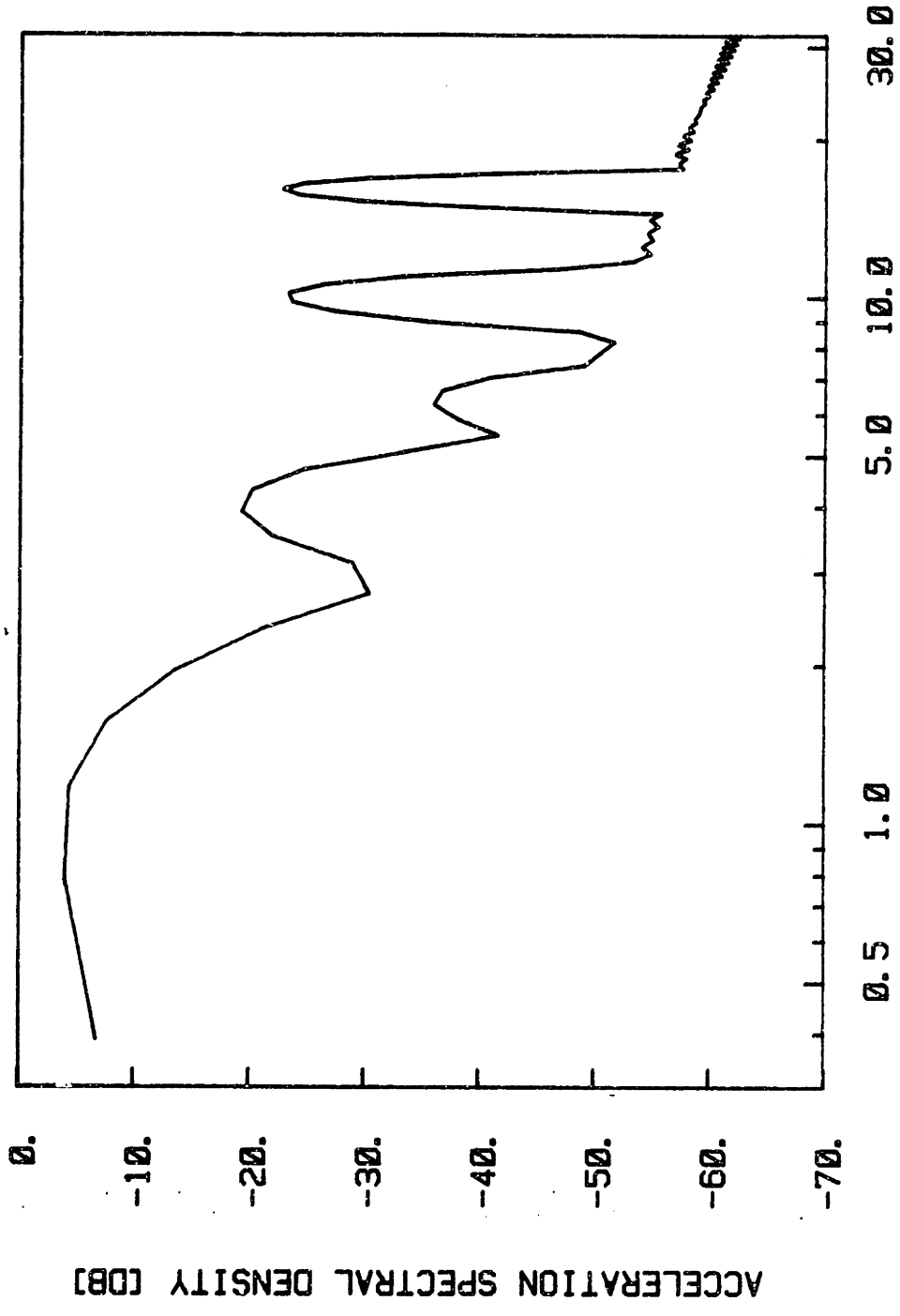

FIGURE 2.4.1 POWER SPECTRAL DENSITY OF AMCOACH LATERAL ACCELERATION.

2.2.2 Valve Dynamics

In order to simulate the air flow through the solenoid valve, an empirical relation [16] was used:

$$\dot{w} = C_1 A_e (P_u/T_u^{1/2})(P_d/P_u)[1 - (P_d/P_u)^{(k-1/k)}] \qquad (2.4.1)$$

for $P_d/P_u \geq 0.528$

and

$$\dot{w} = C_2 A_e (P_u/T_u^{1/2}) \qquad \text{for } P_d/P_u < 0.582 \qquad (2.4.2)$$

where: $\dot{w}$ = weight rate of flow, lbf/sec,

C_d = discharge coefficient of the orifice,

A_e = effective orifice area, in^2,

P_u = upstream stagnation pressure, psia,

P_d = downstream stagnation pressure, psia,

T_u = upstream stagnation temperature, °R.

and for air:

$k = 1.4$

$R = 2.47 \times 10^5$ $in^2/sec^2 °R$,

$C_1 = 2.06$ $°R^{1/2}/sec$,

$C_2 = 0.535$ $°R^{1/2}/sec$.

The opening and closing time delays, were included in the dynamics of the valve as shown in the subroutine VALVE appendix 1. The dynamic of the flow through the valve, is simulated in the subroutine FLOW.

2.2.3 Actuator Dynamics

For the pneumatic cylinder, the weight rate of flow is given by:

$$\dot{w} = g\,\dot{m} = g\,\frac{d}{dt}\,(D_a V_a) \qquad (2.4.3)$$

where: $\dot{m}$ = mass rate of flow, slugs/sec,

g = acceleration of gravity, ft/sec^2,

D_a = air density, $slugs/ft^3$,

V_a = cylinder volume, ft^3.

Assuming that for the operating pressure and temperature the air behaves as an ideal gas,

$$P = D_a R\,T \qquad (2.4.4)$$

where: P = the air pressure inside the cylinder, psia,

T = the air temperature inside the cylinder, °R,

R = the air constant, $ft^2/sec^2{}^\circ R$,

and sustituting equation 2.4.4 in equation 2.4.3, we get:

$$\dot{w} = g\,\frac{d}{dt}\,[(V_a P)/(R\,T)] \qquad (2.4.5)$$

For a polytropic process:

$$P\,D_a^{-n} = \text{constant} \qquad (2.4.6)$$

where n is the polytropic exponent.

Using this equation, the temperature and pressure at any given state can be related to the supply pressure and temperature by the relation:

$$T/P^{(n-1/n)} = T_s/P_s^{(n-1/n)} \qquad (2.4.7)$$

where the s subscript indicates supply conditions.

Substituting the temperature T in equation 2.2.5 and carring out the differentiation:

$$\dot{P} = (n\ R\ T_s/V_a g)(P_s/P)^{(n-1/n)}\dot{w} - (n\ P/V_a)\dot{V}_a \qquad (2.4.8)$$

In this equation, $\dot{w}$ is given by equation 2.4.1 or 2.4.2, while V_a and $\dot{V}_a$, can be calculated as a function of the cylinder stroke as follows:

$$V_a = A_p(Yt-Yc) + V_o \qquad (2.4.9)$$

where: A_p = piston area, in^2,

V_o = initial piston volume, in^3,

so that:

$$\dot{V}_a = A_p(\dot{Y}t-\dot{Y}c) \qquad (2.4.10)$$

Integration of equation 2.4.8 gives the pressure in the pneumatic cylinder. The force produced by the actuator can be calculated as:

$$Fa = A_p P \qquad (2.4.11)$$

Since two actuators are being used, the resultant net force must be calculated. Using this resultant force, and equation 2.2.5, the dynamics of the one degree of freedom model can be completely described.

2.2.4 Power Consumption

For a steady state flow process, the specific work done by the compressor can be calculated as:

$$W = \int_i^e dP/D_a \qquad (2.4.12)$$

where i and e denote inlet and exit conditions. If an isothermal process is assumed, Eq. 2.4.12 becomes:

$$W = R\ T_i Ln(P_e/P_i) \qquad (2.4.13)$$

If an isentropic process is assumed, eq. 2.4.12 becomes:

$$W = (k/k-1)R\ T_i [(P_e/P_i)^{(k-1/k)} - 1] \qquad (2.4.14)$$

where k is the ratio of specific heats.

Equations 2.4.13 and 2.4.14, give the upper and lower estimate of the work done by the compressor.

Chapter 3

EXPERIMENTAL SET UP AND MODEL EVALUATION

3.1 INTRODUCTION

A set of experiments were performed to evaluate the accuracy of the equations presented in chapter two, when applied to describe the dynamics of the active pneumatic suspension components. In these tests, the open loop step response, and the closed loop frequency response of a solenoid valve-pneumatic actuator assembly were studied. The results obtained were used to evaluate, in an economical and simple manner, the feasibility of using the proposed control law in a active pneumatic suspension system.

The "static response" of the system was evaluated to determine the characteristics of solenoid valves and pneumatic actuators. This was accomplished by using a pneumatic actuator with its attachment points connected to the ground. Since the actuator was not allowed to move, the complete dynamics of the system was not experimentally studied. The results obtained, however, allowed the partial verification of

the model used. They also gave information that could be utilized for the setting up of a prototype system that would allow a complete experimental evaluation of pneumatic active suspensions.

In this chapter, the hardware considerations regarding the experimental studies performed are presented. The experimental results are compared to those obtained by using computer simulation, and the discrepancies are explained.

3.2 ELECTRICAL HARDWARE DESIGN

A laboratory electrical circuit, capable of generating the desired control signal, was built to implement the control law given in Fig. 2.3.1. This circuit, was designed to withstand the severe working conditions that could be generated in the different tests performed [14]. In this circuit, the desired force Fd, and the actual actuator force Fa, were used as inputs to generate the control signal Vc. Since acceleration feedback from the mass was not possible, calculation of the desired force Fd, was not required. For this reason, the hardware necessary for the calculation of the desired force was not included in the circuit.

De Los Reyes [14], built an analog circuit that allows the calculation of the desired force Fd as a function of the

accelerometer output, $\ddot{Y}c$. This circuit and the one developed in this research could be coupled to generate the control signal Vc required for the dynamic testing of an active pneumatic suspension device.

Figure 3.2.1 shows a detailed electrical schematic of the controller used to drive the experimental apparatus. This schematic has been divided into four different operational blocks. Each of these blocks is used to perform one of the different operations of the controller.

In block A, the desired and actual actuator force are compared, and the error signal, E, is generated. Choosing the signal coming from one of the load cells to represent a "positive" force, and the other, a "negative" force, the net actuator force can be obtained as the sum of these two signals. The error signal can be calculated by adding the resultant actuator force to the desired actuator force.

The "compensated error", Ec, is generated in block B. In this part of the circuit, one operational amplifier is used to invert the error signal, and a second is used to perform the differentiation. The "compensated error", Ec, is obtained by summing these two signals. Active differentiation was used for the calculation of the derivative of the error because it gave good results for low frequency signals. The low pass filter required to attenuate high frequency noise was not included in the circuit since for the test conditions it was

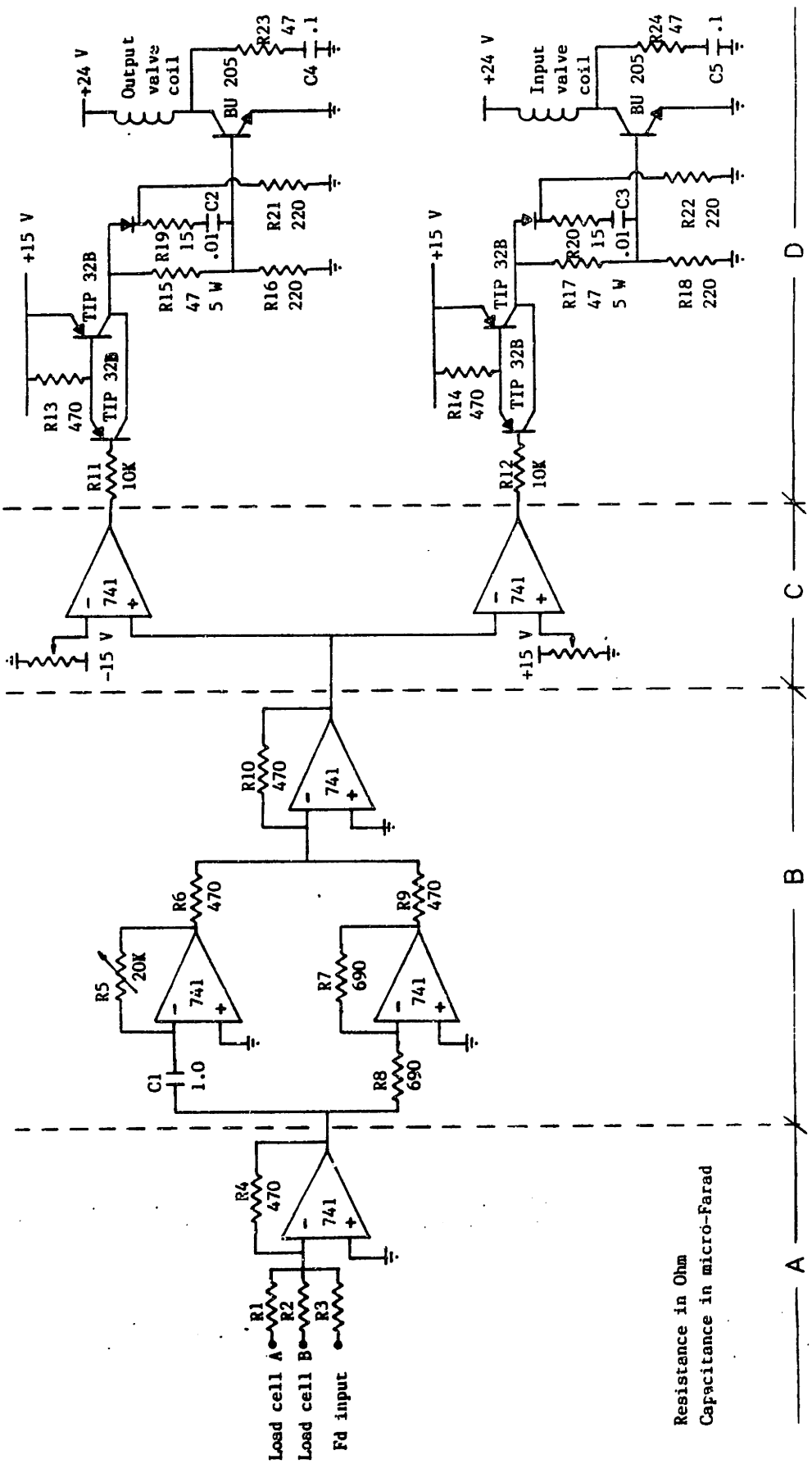

FIGURE 3.2.1 ELECTRICAL SCHEMATIC OF CONTROLLER.

not necessary.

Block C is a comparator where the "compensated error" is compared to two reference voltages that define the width of the dead zone. Two voltage dividers were used to set these reference voltages. The result of this comparison is a continuous voltage of 15, 0 or -15 volts that is used to trigger the output switching transistors of the circuit.

In block D, the signal coming from block C, is amplified so that it can be used to drive the input and output solenoid valves. High voltage switching transistors were required in the last step of amplification in order to increase the bandwidth of the valves. Because the current in the coil of the solenoid valves can not be cut off instantaneously, each time the transistor is switched off, a large voltage is generated in the coil. An RC circuit between the collector of the transistor and ground was used to reduce these high voltage signals, at the expense of increasing the time required by the solenoid valve to close.

Several tests were performed to verify the performance of the circuit. Figure 3.2.2 shows a sinusoidal input signal of 1 hz and its derivative as obtained by using active differentiation. In this example, the derivative gain, T, was set to 0.014. For this low frequency, typical in active suspension systems, the differentiation can be performed with very good results.

INPUT AND OUTPUT VOLTAGES
[1 VOLT/DIV.]

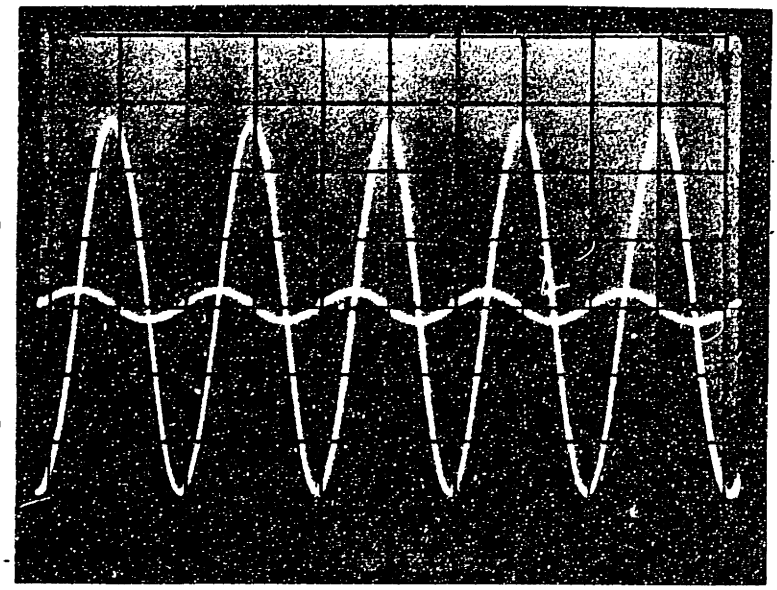

TIME [0.5 SEC/DIV.]

FIGURE 3.2.2 ACTIVE DIFFERENTIATION.

Figure 3.2.3 shows the step response of the electrical circuit when connected to the coil of the solenoid valve. As it is shown, the coil could be energized to open the valve at very high speed. De-energize the coil to close the valve was, however, a much slower process. This was due to the dynamics of the coil. Decreasing the time required to de-energize the coil implies increasing the voltage through the switching transistor. This creates a trade-off between the maximum voltage across the transistor and the time required by the solenoid valve to close.

3.3 EQUIPMENT SET UP

For the experimental evaluation of the response of the solenoid valve/pneumatic actuator assembly, a 4 inch pneumatic cylinder and two Festo MX-2-1/4 2/2 way solenoid valves were used. Only one actuator was used to determine the characteristics of the valve and pneumatic cylinder.

Festo MX-2-1/4 solenoid valves were chosen for their peak and nominal flow rate of 143 and 54 scfm respectively, and their relative high bandwidth (see specifications appendix 4). The 4 inch bore pneumatic actuator was chosen since studies done in proportional pneumatic active suspensions [13] have shown that this type of actuators could be successfully

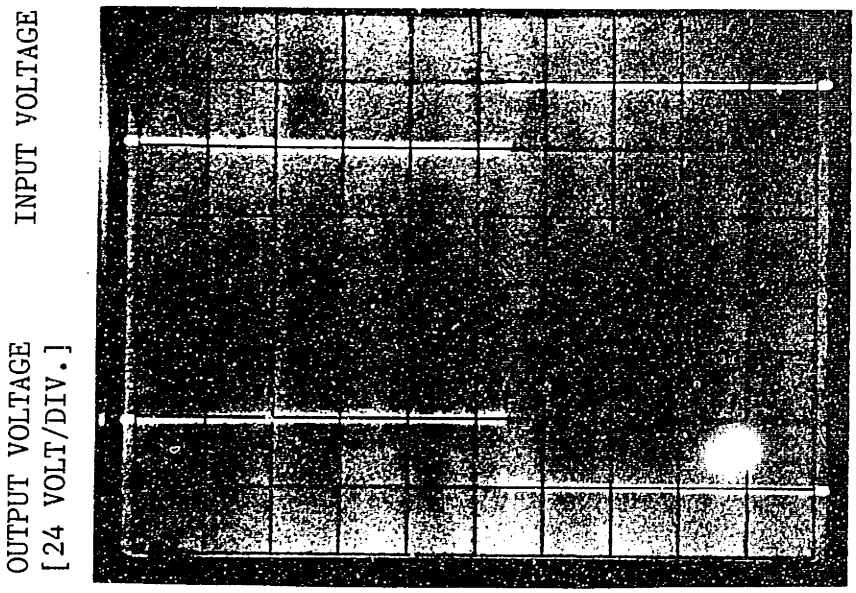

TIME [0.02 SEC/DIV.]

Step response to an open command

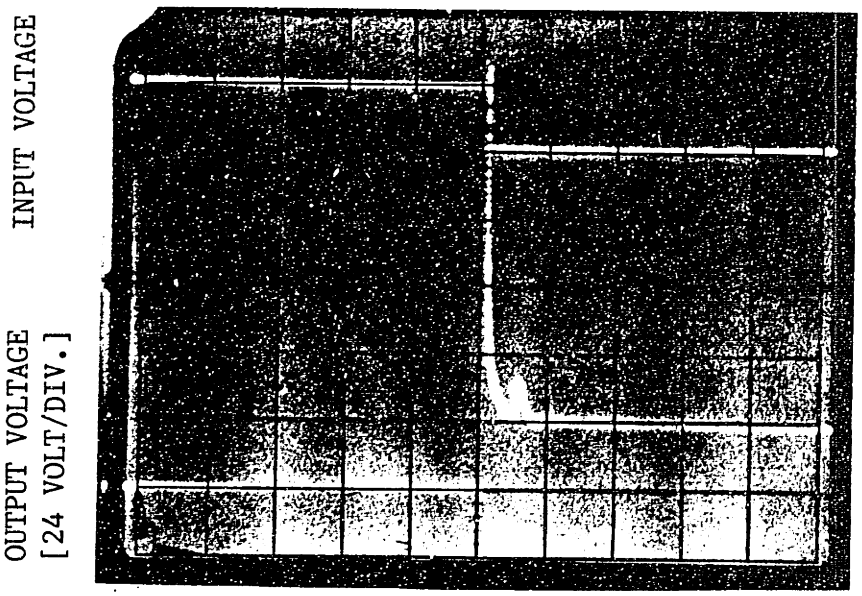

TIME [0.02 SEC/DIV.]

Step response to a close command

FIGURE 3.2.3 ELECTRIC CIRCUIT STEP RESPONSE.

used to reduce lateral acceleration of rail vehicles with a relatively low power consumption.

The desired force, used as the input in this system, was simulated using a signal generator. The actual actuator force, required to close the feedback loop, was obtained from a load cell placed between the shaft of the pneumatic actuator and ground. An oscilloscope was used in order to determine the response of the system. Measuring the actual actuator force coming from the load cell, and the desired input force comming from the signal generator, the characteristics of the valve/cylinder assembly could be evaluated.

4.4 MODEL EVALUATION

To verify the accuracy of the digital model in simulating active pneumatic suspensions, the testing of the valve/cylinder assembly was divided into two parts. The "static testing" or open loop step response of the system, and the "dynamic testing" or closed loop response of the system to sinusoidal inputs. The FORTRAN subroutine MODEL (appendix 1) was used throughout this model verification. The numerically integration of the differential equations that describe the system were performed using a fourth order Runge-Kutta routine.

To determine the opening and closing pure time delays of the solenoid valves, the response of the system to a step input in the desired force was evaluated. With a supply pressure of 120 psig, the input valve of the pneumatic cylinder was opened while keeping the output valve closed. Figure 3.4.1 shows that a pure time delay of 22 ms. was present in the response of the system.

To determine the closing time delay of the solenoid valve, the input valve of the pneumatic actuator was briefly opened, while keeping the output valve closed. When the air flow through the valve was established, a close command for that valve was generated. As shown in Fig. 3.4.2, the time required for the solenoid valve to close, including electrical and mechanical delays, was about 60 ms.

According to the valve and solenoid specifications, the total opening and closing time delays are 34 and 26 ms respectively. Although several tests were performed, these specified values could not be met. These discrepancies were attributed to the different testing procedures used to determine the response of the valve. The values obtained in this test were used in the digital simulation since, for the operation conditions of the system, they represent a more accurate estimate of the opening and closing time delays of the valve.

For a supply pressure of 80, 100 and 120 psig, the

FORCE [212 LBF/DIV.]

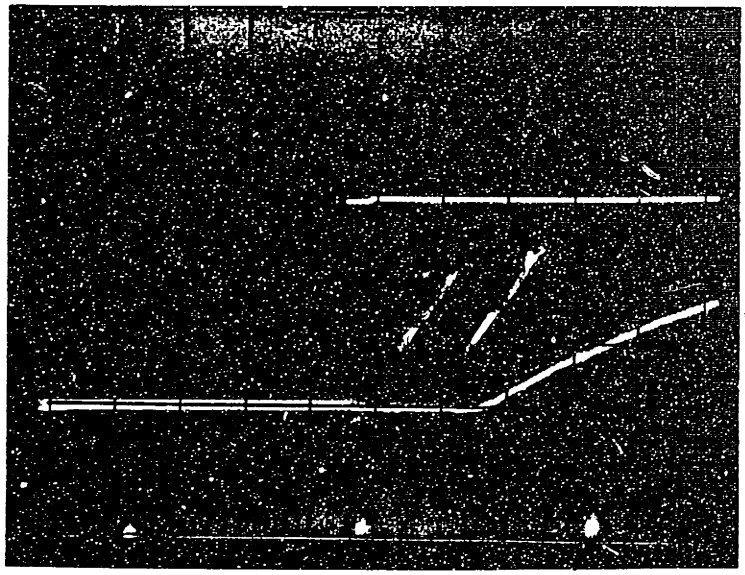

TIME [0.01 SEC/DIV.]

FIGURE 3.4.1 VALVE OPENING PURE TIME DELAY.

FORCE [212 LBF/DIV.]

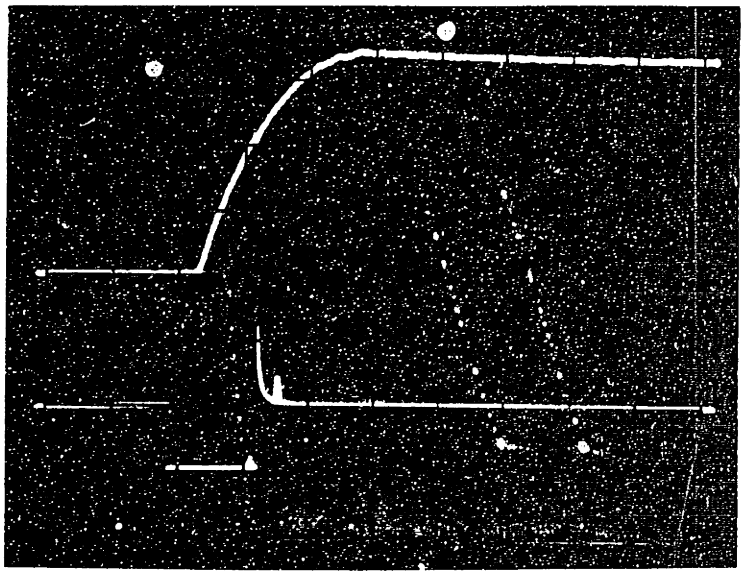

TIME [0.05 SEC/DIV.]

FIGURE 3.4.2 VALVE CLOSING PURE TIME DELAY.

step response of the system for the filling and exhausting process were evaluated. For a nominal "height" of the actuator fixed to 4 inches, the pressure inside the cylinder was stepped up from the atmospheric pressure to the different supply pressures. This was done by opening the input valve, while keeping the output valve closed. To evaluate the exhausting step response of the assembly, the pressure inside the cylinder was first set to the different supply values, and then the output valve was opened, while keeping the input valve closed.

Modeling the valve with an effective orifice area of 0.06 square inches, and assuming that the process is isothermal, the experimental results and the calculated values, obtained by using digital simulation, matched well for all the tested cases. Figures 3.4.3 and 3.4.4 show the step response of the valve/cylinder assembly for the filling and exhausting process, and the responses obtained by the digital model for a supply pressure of 120 psig.

A sinusoidal input in the desired force was used to test the closed loop response of the system. For frequencies ranging from 0.1 to 5 hz and different input amplitudes the response of the assembly was studied. In all cases, the supply pressure was set to 120 psig., and the nominal actuator height was fixed to 4 inches. Figures 3.4.5 to 3.4.10 show the closed loop frequency response of the experimental

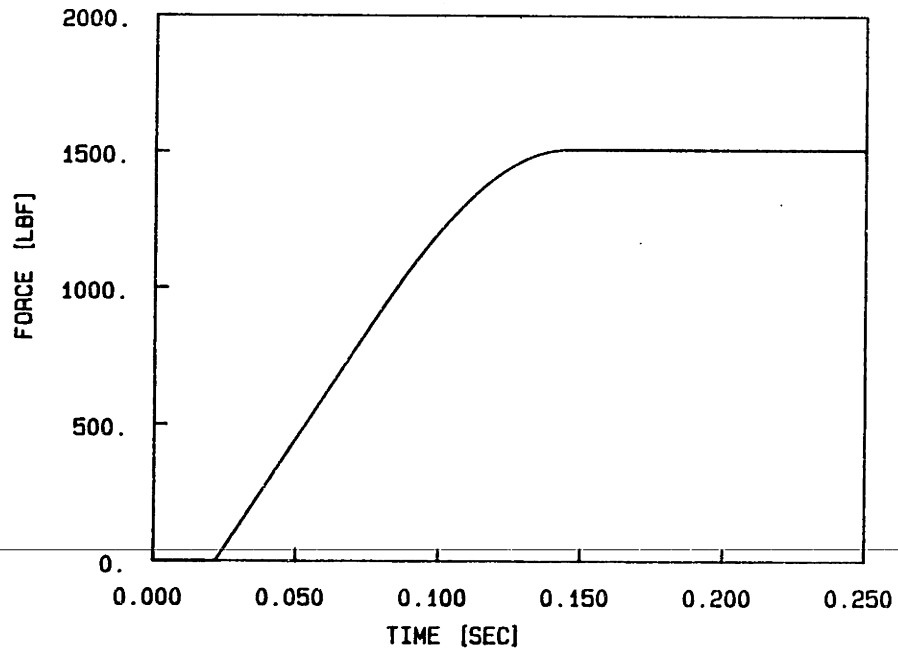

Model response

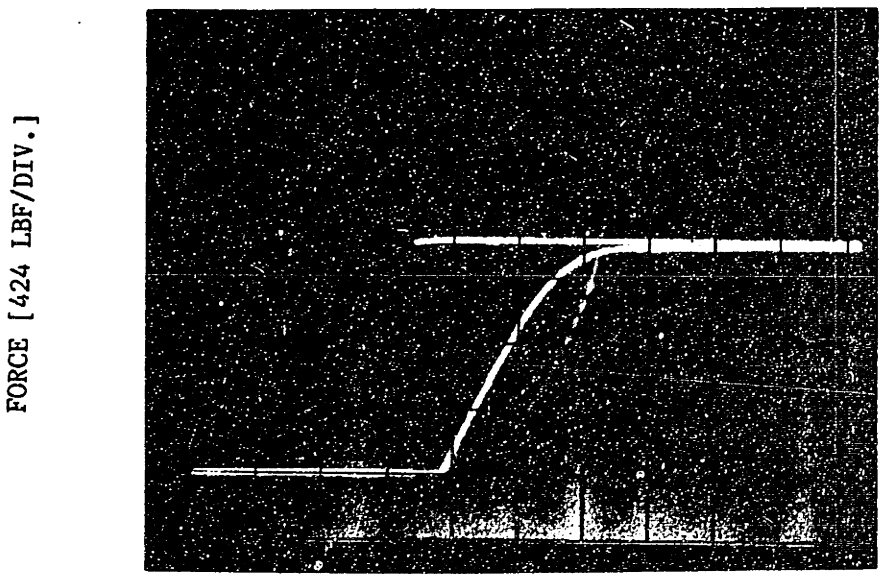

TIME [0.05 SEC/DIV.]

Experimental result

FIGURE 3.4.3 OPEN LOOP FILLING STEP RESPONSE.

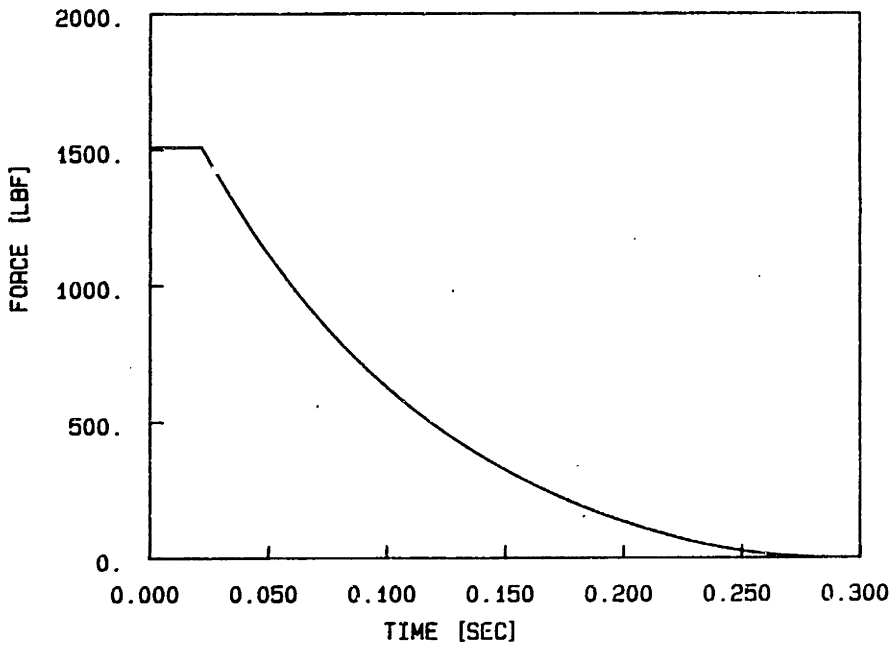

Model response

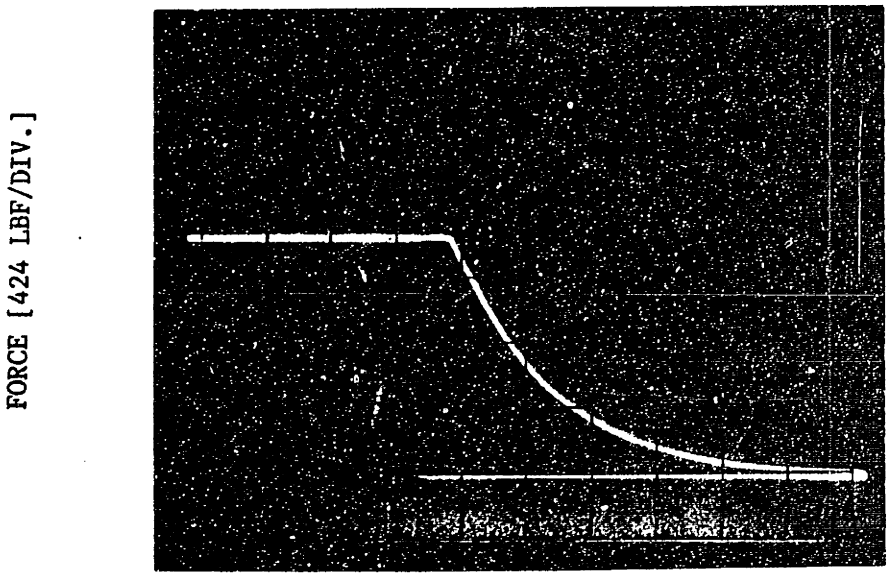

TIME [0.05 SEC/DIV.]

Experimental result

FIGURE 3.4.4 OPEN LOOP EXHAUSTING STEP RESPONSE.

apparatus, and the closed loop response obtained by using the implemented program for frequencies of 0.1, 1, 2, 3, 4 and 5 hz, and an input amplitude of 1500 lbf. Only "positive" actuator forces could be generated since only one actuator was used. For this reason, the actual actuator force went to zero when the desired force was negative. In a real system implementation, two actuators would be used to generate positive and negative forces. With this configuration, the response of the system would be faster, since the exhausting process of one cylinder would be helped by the filling process of the other.

Figures 3.4.5 to 3.4.10 show that for low frequencies, 0.1 to 1 hz, the model is a very good approximation of the experimental system. As the frequency is increased, the discrepancies become more noticeable. These differences are primarily due to the fact that the output valve of the cylinder opened for a brief period of time when the air was filling up the cylinder. It is for this reason that at high frequencies the attenuation of the tested system is larger than that of the simulated system. This effect was not included in the model, since it was assumed that an output valve which will not open as a result of sudden changes in the cylinder's pressure can be found.

The response of the experimental system for frequencies larger than 3 hz, shows that a noticeable phase

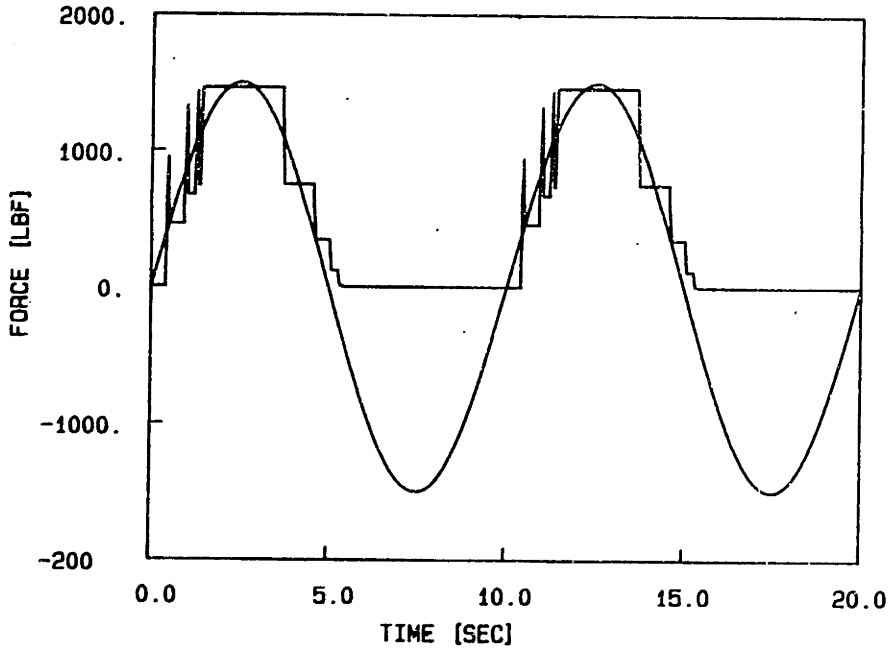

Model response

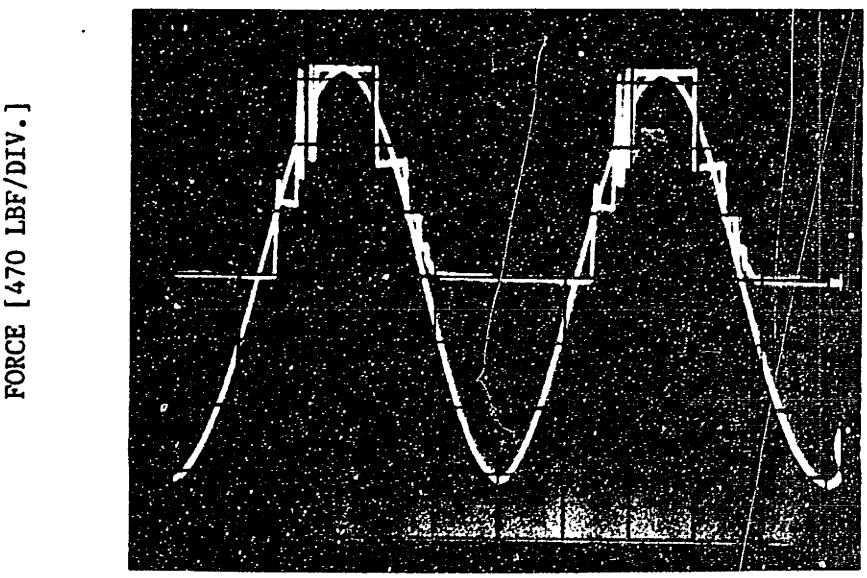

Experimental result

FIGURE 3.4.5 CLOSED LOOP FREQUENCY RESPONSE
W = 0.1 HZ.

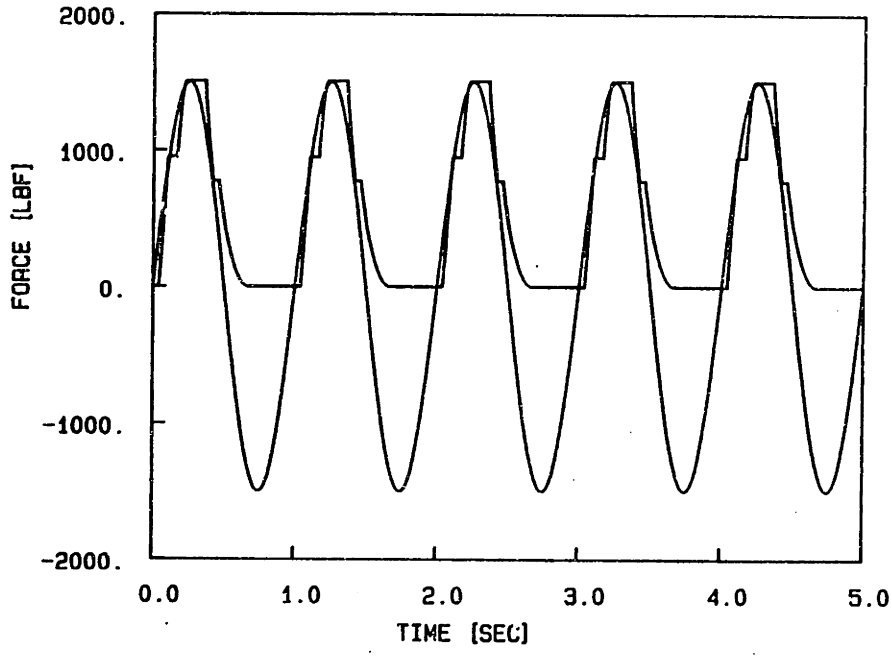

Model response

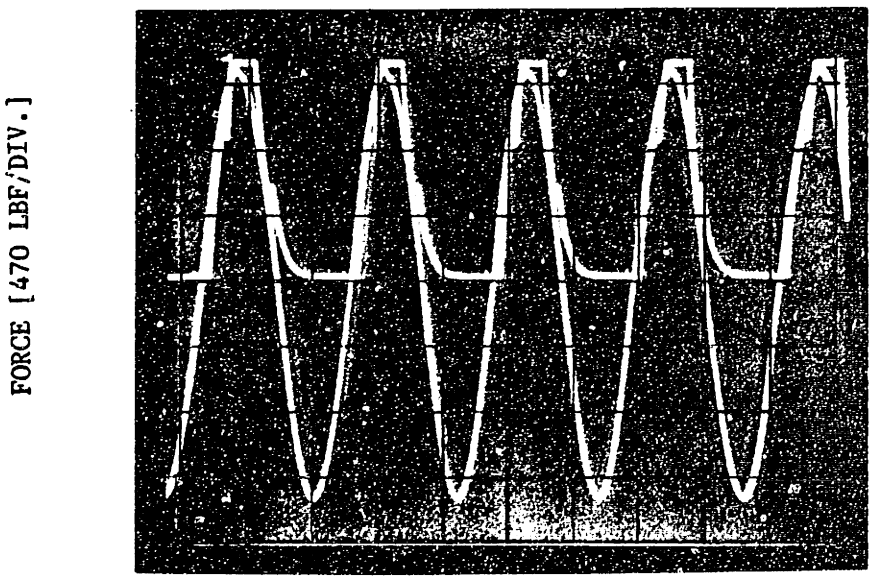

TIME [0.5 SEC/DIV.]
Experimental result

FIGURE 3.4.6 CLOSED LOOP FREQUENCY RESPONSE
W = 1.0 HZ.

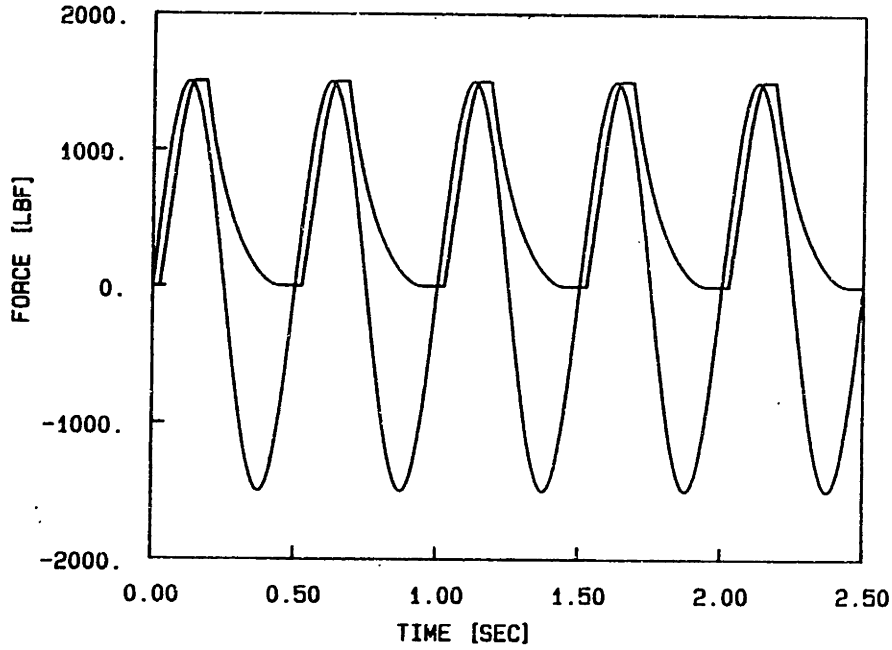

Model response

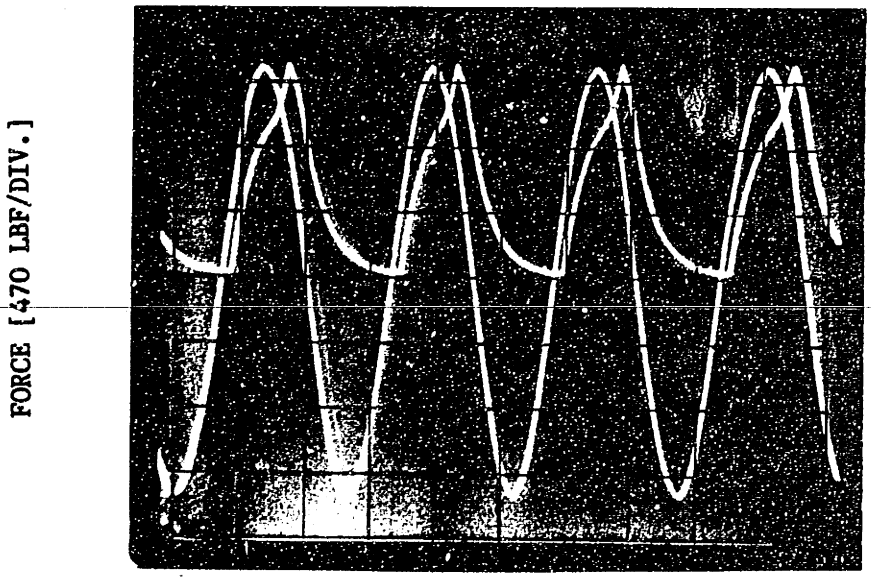

TIME [0.2 SEC/DIV.]

Experimental result

FIGURE 3.4.7 CLOSED LOOP FREQUENCY RESPONSE
W = 2.0 HZ.

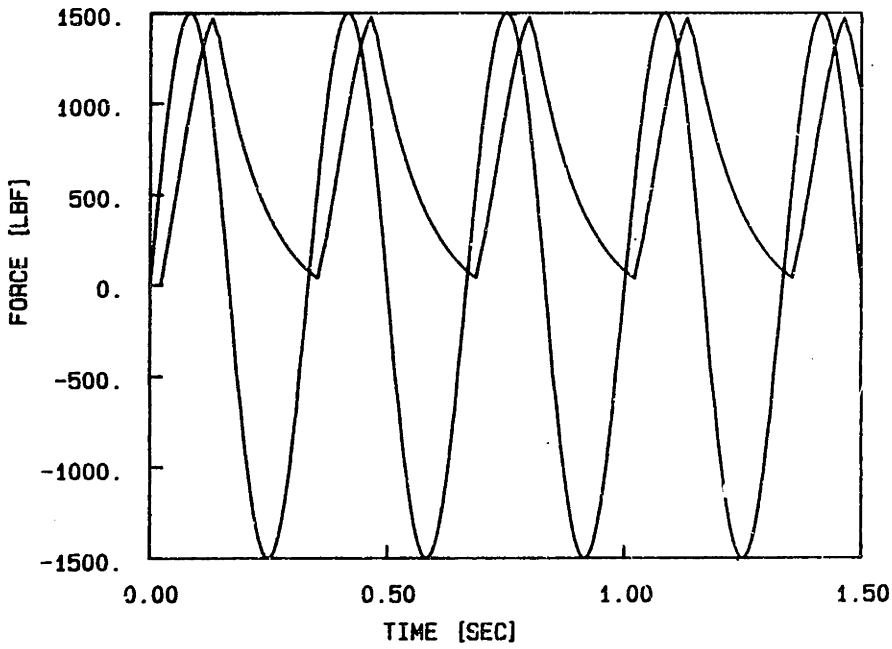

Model response

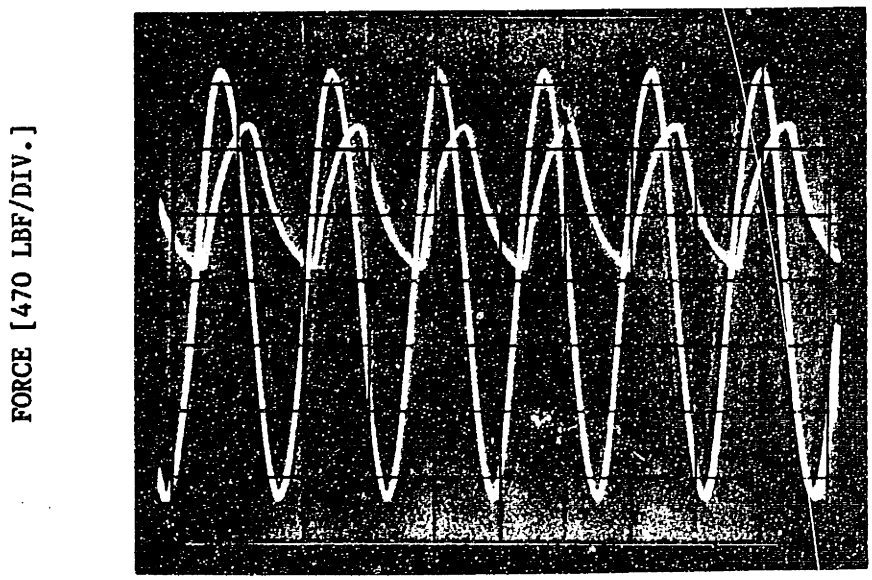

Experimental result

FIGURE 3.4.8 CLOSED LOOP FREQUENCY RESPONSE
W = 3.0 HZ.

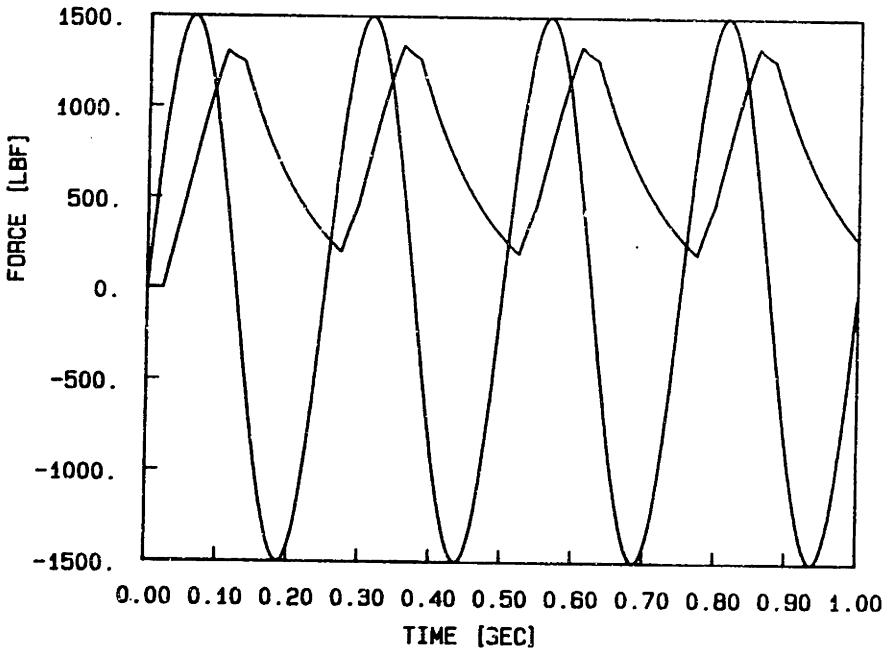

Model response

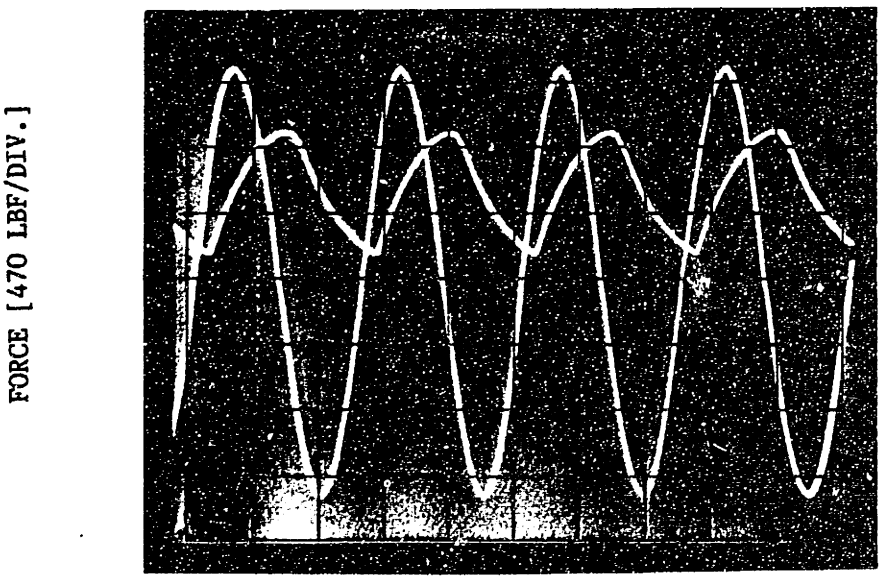

TIME [0.1 SEC/DIV.]

Experimental result

FIGURE 3.4.9 CLOSED LOOP FREQUENCY RESPONSE

W = 4.0 HZ.

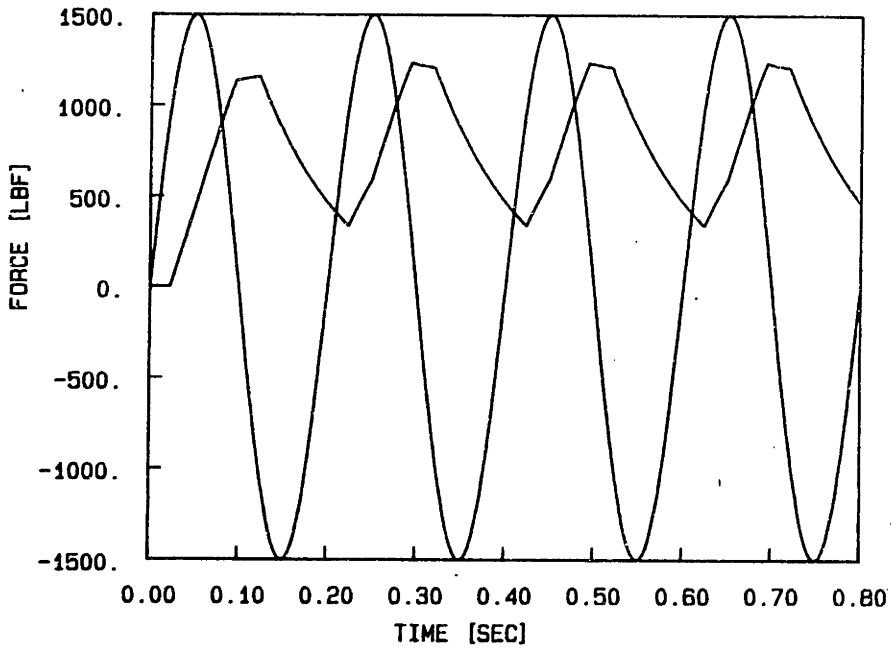

Model response

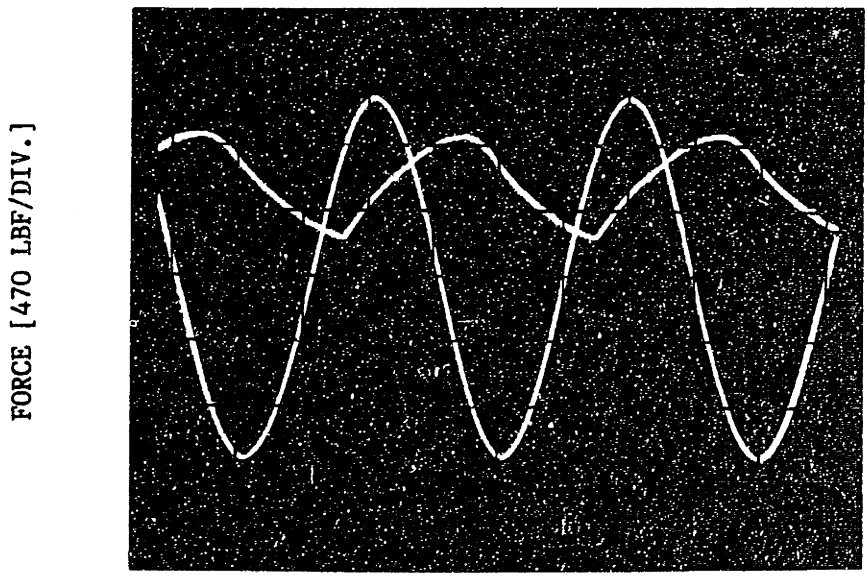

Experimental result

FIGURE 3.4.10 CLOSED LOOP FREQUENCY RESPONSE
W = 5.0 HZ.

lag is present. For this range of operation, the desired and actual actuator force could have opposite signs, affecting the performance of the active suspension system. To eliminate this problem, a low pass filter could be used to avoid system responses above 3-4 hz.

The tests performed thus far have shown that the model used to simulate the valve/cylinder assembly can be satisfactorily utilized to describe the static response of the system. In the following chapter, this model is used to predict the performance of nonlinear active pneumatic suspensions, when used on rail vehicles.

Chapter 4

PERFORMANCE OF ACTIVE PNEUMATIC SUSPENSIONS

4.1 INTRODUCTION

A one degree of freedom model for the carbody lateral dynamics and the equations given in chapter two, for the different active suspension components, were used to determine the effectiveness of pneumatic active suspensions when applied to increase ride the quality performance of rail vehicles. Although these equations represent a simplification of the real system dynamics, their use allowed a preliminary quantitative description of the system, which could be utilized to define some of the most important characteristics of the active suspension proposed.

In rail vehicles, ride quality is normally taken to be a measure of passenger comfort. This is a highly subjective opinion based on many parameters. The most significant of these parameters which is directly affected by the suspension is the level of vibration in the passenger compartment. When active suspension systems are evaluated, the carbody stroke

and the power required by the suspension system, become important parameters which should be considered as part of a complete description of the system performance.

In this study, the ride quality and active suspension performance were measured as a function of the root mean square (r.m.s.) carbody lateral stroke and acceleration, the carbody acceleration power spectral density, and the average power consumption. Since pseudo-random disturbances were assumed, the r.m.s. carbody lateral stroke and acceleration were used as representative indices of the "overall" stroke and acceleration of the passenger compartment. The r.m.s. values, however, do not give any information about the frequency content of the response. Since human body sensitivity to lateral acceleration is a function of the frequency, the acceleration power spectral density was also used as a performance index. The operation costs of active suspension systems, are largerly related to their power consumption. This parameter was, therefore, used to evaluate the economical aspects of the active suspension systems.

4.2 RIDE QUALITY PERFORMANCE

In the evaluation of the performance of active pneumatic suspensions, the baseline parameters of an Amtrak passenger-coach were used as an example (Table 2.1). Figure

4.2.1 shows the acceleration and acceleration power spectral density response of the passive system when using the proposed disturbance input. For this case, in which no active elements were used, the peak acceleration was 0.170g, and the r.m.s acceleration was 0.070g. The peak stroke was 1.430 inches, and the r.m.s. stroke was 0.640 inches.

The performance of an ideal active suspension are shown in Fig. 4.2.2. The response of the system, when using ideal actuators, could be evaluated by making the actuator force, Fa, equal to the desired force, Fd. Using an acceleration feedback gain, K1, of 20 lbf-sec^2/in and a velocity feedback gain, K2, of 1800 lbf-sec/in, the r.m.s. acceleration could be reduced by 74% to 0.018g, and the r.m.s. stroke could be reduced by 22% to 0.498 inches. The r.m.s. lateral carbody acceleration could be further reduced by increasing the acceleration or velocity feedback gain, at the expense of a larger r.m.s. stroke. Design constraints require the r.m.s. stroke to be less than 0.5 inches, making larger reductions impossible.

The subroutine SYS (appendix 2) was used to simulate the response of the system when using the active pneumatic suspension system proposed in this thesis. Using two 4 inch bore pneumatic cylinders as actuators, and four Festo MX-2-1/4 solenoid valves, the r.m.s carbody lateral acceleration of the baseline system could be reduced by 49% to 0.0355g and the

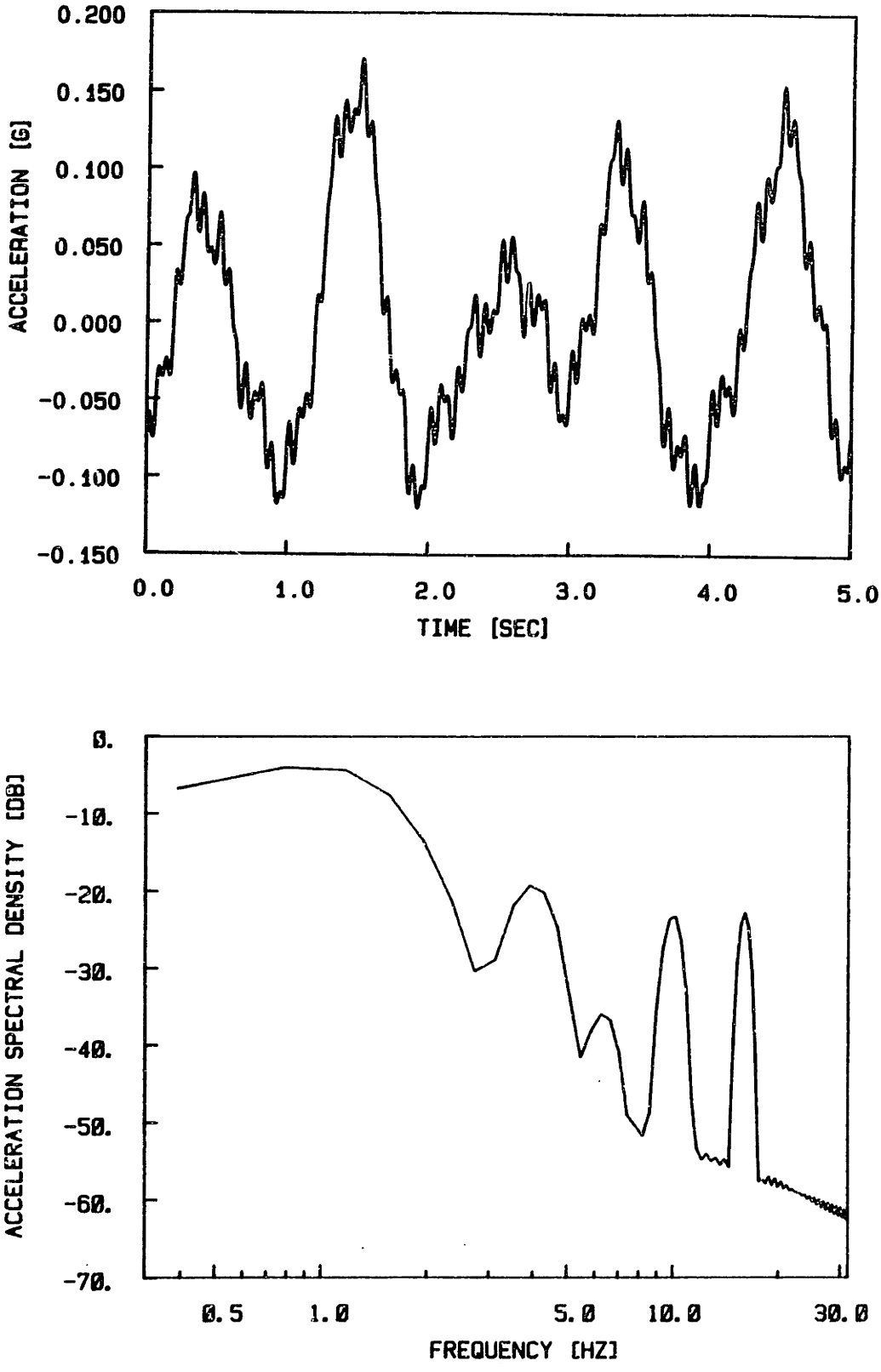

FIGURE 4.2.1 PASSIVE SYSTEM ACCELERATION RESPONSE.

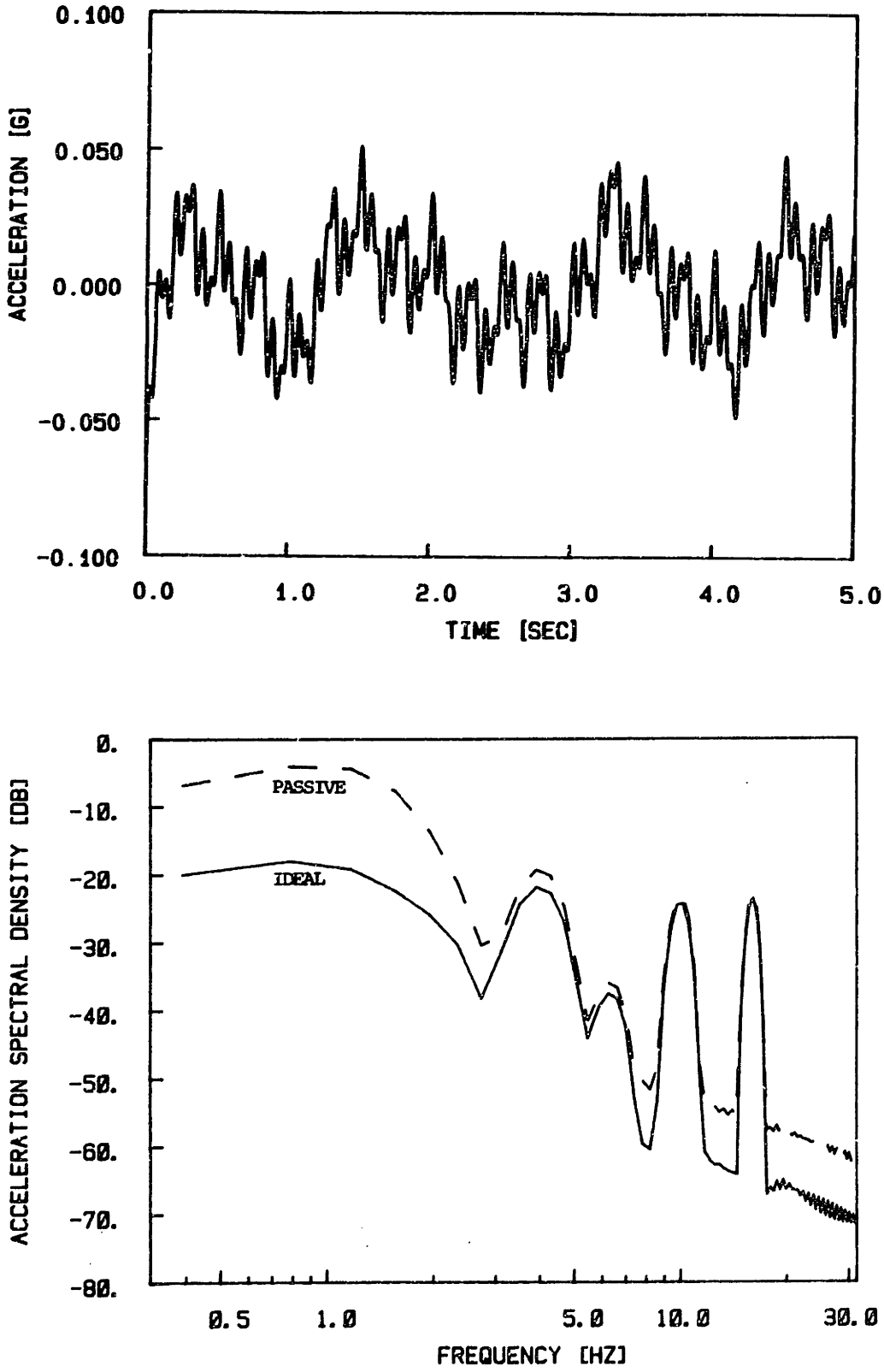

FIGURE 4.2.2 IDEAL ACTIVE SYSTEM ACCELERATION RESPONSE.

r.m.s. stroke could be reduced by 30% to 0.448 inches. After a trial and error process, in which the r.m.s. acceleration was minimized, the optimal parameters of the controller were found to be: 15 lbf-sec^2/in for the acceleration feedback gain, K1; 2400 lbf-sec/in for the velocity feedback gain, K2; 0.014 sec. for the "lead time", T; and 300 lbf for the "dead zone width", Fr.

Figure 4.2.3 shows the carbody lateral stroke for 5 seconds of simulation. The peak stroke was 0.855 inches, which is 57% of the allowable maximum peak value of 1.5 inches. Thus for the simulated input, no contact between the carbody and the bumpstops occured when the active suspension was used.

Figure 4.2.4 shows the desired and actual actuator force for this case. For the 4 inch bore actuators used, the affective piston area is 12.56 square inches. With a supply pressure of 130 psig, the maximum force that can be produced by the actuator is 1634 lbf. Although this maximum force is a small fraction of the maximum desired force, the simulation showed that good performance could still be obtained. It should be noted, that the desired force for this case was larger that the one used for the ideal case. This was due to the fact that increasing the velocity and acceleration feedback gains, a "smoother" actuator response could be obtained, which reduces the low frequency oscillations in the

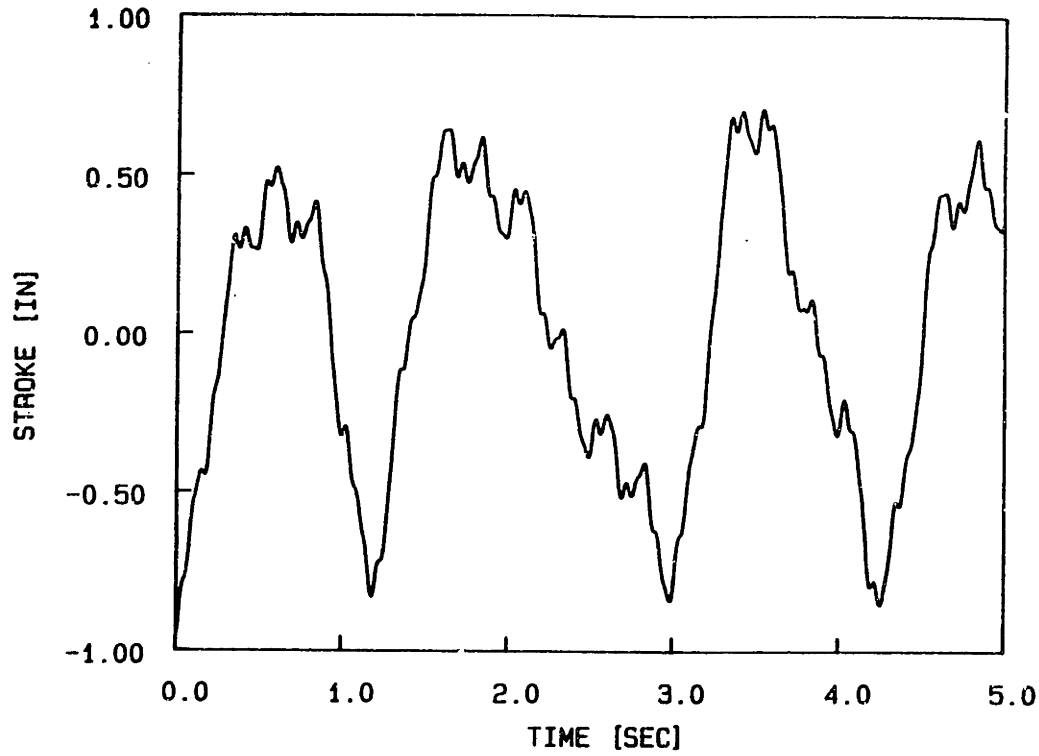

FIGURE 4.2.3 ACTIVE SYSTEM SUSPENSION STROKE.

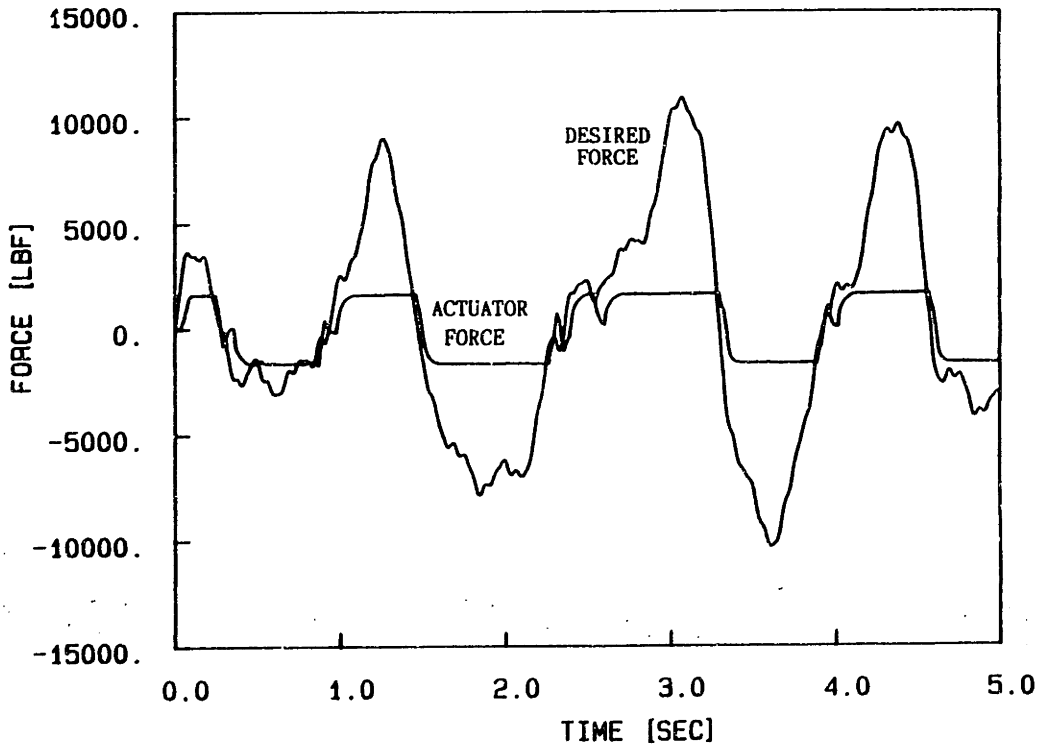

FIGURE 4.2.4 ACTIVE SYSTEM DESIRED AND ACTUAL ACTUATOR FORCE.

acceleration response. Figure 4.2.4 also shows that when the actuator force was not clipped at 1634 lbf, the actual actuator force followed the desired force without any significant lag.

Figure 4.2.5 shows the carbody lateral acceleration as a function of time, and its power spectral density as compared to the passive case. A substantial reduction was provided in acceleration vibration. The peak carbody lateral acceleration for this case was 0.114g, which is the 33% of the peak acceleration of the passive case. For frequencies below 2 hz, the acceleration was attenuated by approximately 8 db. For higher frequencies, however, the active suspension system degraded the system response. This is a result of the low bandwidth of the solenoid valve/pneumatic cylinder assembly. If better performance at high frequencies are desired, faster actuators must be used. The high frequency response, however, has little influence on the overall effectiveness of the active suspension. The spectral power of the high frequency, is at least 10 db lower than that of the low frequency acceleration. Moreover, the human body is less sensitive to high frequency accelerations (Fig. 1.1.3) and, therefore, their effects in ride quality are not as important.

The average air flow required for the active suspension system during this simulation was 32.85 scfm/truck. This gives a compressor power requirement of 9.5

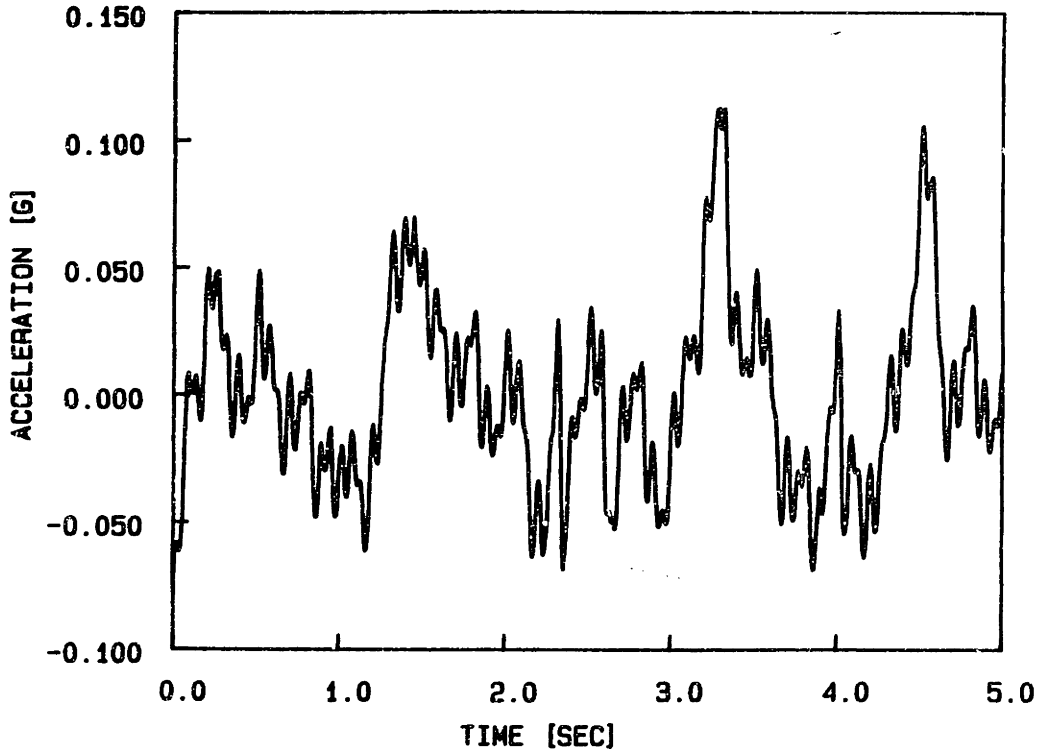

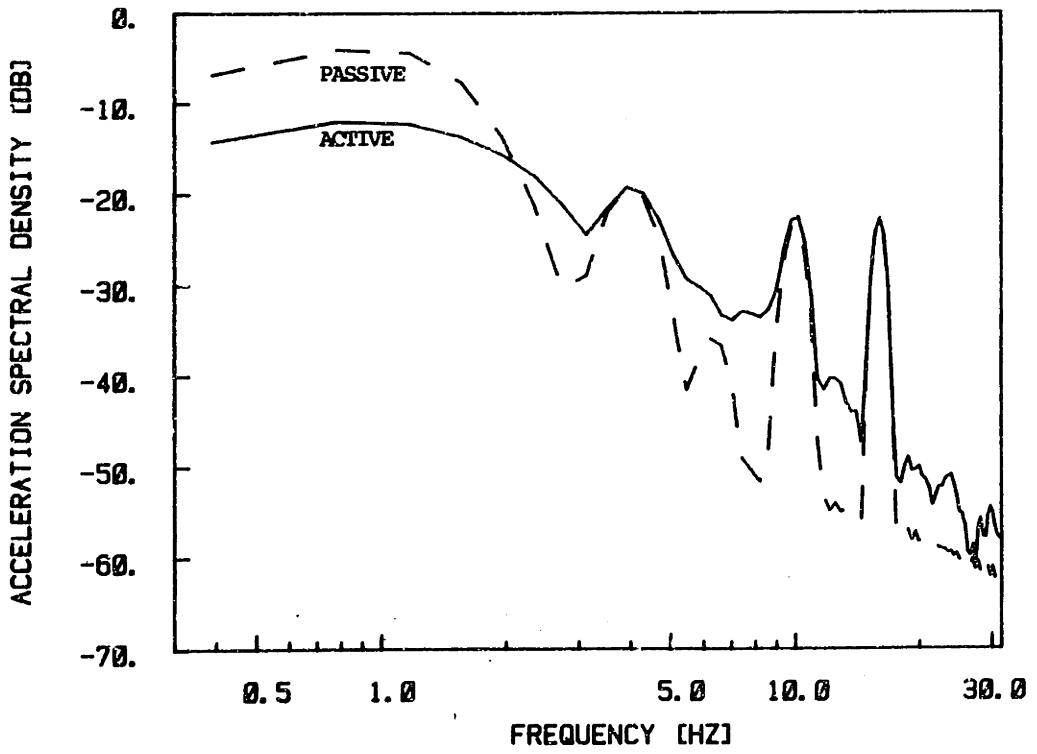

FIGURE 4.2.5 ACTIVE SYSTEM ACCELERATION RESPONSE.
BASELINE PARAMETERS.

to 13.3 horsepower/car. For a typical 10 car passenger train, this means that a compressor of at least 133 hp has to be used. This power requirement is not very high and it can be easily supplied by an onboard compressor.

Changes in the baseline system stiffness and damper coefficients were proposed to further decrease the r.m.s. carbody lateral acceleration. As the spring stiffness was decreased, better performance in the acceleration response could be achieved, at the expense of a higher power consumption. Changes in the damping coefficient, on the other hand, had very little effect on the system response. Figure 4.2.6 shows the system acceleration response and its power spectral density when using the proposed active suspension system in parallel with a 3000 lbf/in spring and the baseline damper. The stiffness used for this simulation was the minimum value that could be used while meeting the static displacement specifications. For this case, the lateral carbody r.m.s acceleration was reduced by 60% to 0.0278g, and the r.m.s. stroke was reduced by 22% to 0.499 inches. The power consumption, however, was increased from 9.5-13.3 hp./car, for the baseline parameters, to 15-21 hp/car. This higher power consumption and the fact that changing lateral stiffness involves a high initial installation cost, makes the use of this configuration unattractive.

Table 4.1 summarizes the results obtained in this

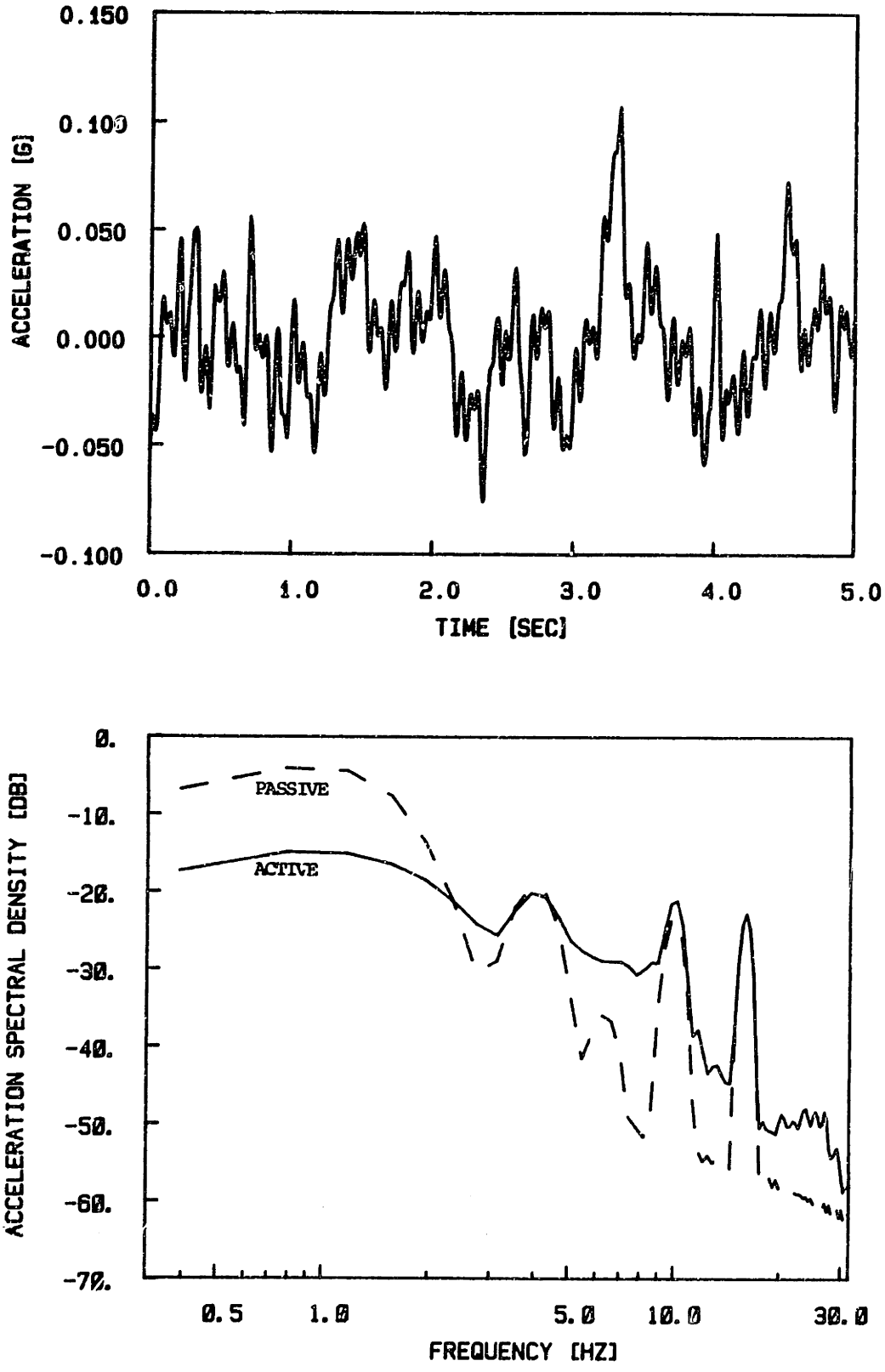

FIGURE 4.2.6 ACTIVE SYSTEM ACCELERATION RESPONSE.
MODIFY PARAMETERS.

section. Fig. 4.2.7 shows a comparison of the acceleration power spectral density of the passive case, the active case using the baseline parameters and pneumatic actuators, and the ideal case obtained by assuming ideal actuators. These results show that active pneumatic suspensions driven by the proposed on-off controller perform well for frequencies below 2 hz with a relatively low power consumption.

Cho [13], showed that using a proportional valve with a peak flow capability of 40 scfm, and 4 inche bore pneumatic cylinders, a 46% reduction in the r.m.s. acceleration and 34% reduction in the r.m.s. stroke can be achieved while using only 5.4-7.6 horsepower/car. However, the high cost of proportional valves and their poor reliability, make the nonlinear active pneumatic suspension, studied in this thesis, a very promising alternative to be considered as a mean of improving the ride quality performance of rail vehicles.

4.3 PARAMETRIC STUDIES

For a final design of an active pneumatic suspension system, the influence of changing the different parameters involved should be evaluated. Some of these parameters, such as feedback gains, lead time compensation, and dead zone width, can be easily changed even in an operating system by tuning the controller. However, the actuator diameter, the

Case	A	B	C	D	E
Passive	0.070	0.64	-	-	-
Active (baseline parameters)	0.035	0.45	49	30	9.5-13.3
Active (modify parameters)	0.028	0.49	60	22	15-21
Ideal	0.018	0.49	74	22	-

A = R.M.S carbody acceleration, g;

B = R.M.S. secondary suspension travel, in;

C = R.M.S acceleration change from passive, %;

D = R.M.S secondary suspension travel change from passive, %;

E = power consumption, Hp/truck.

Table 4.1.- ACTIVE SUSPENSION PERFORMANCE

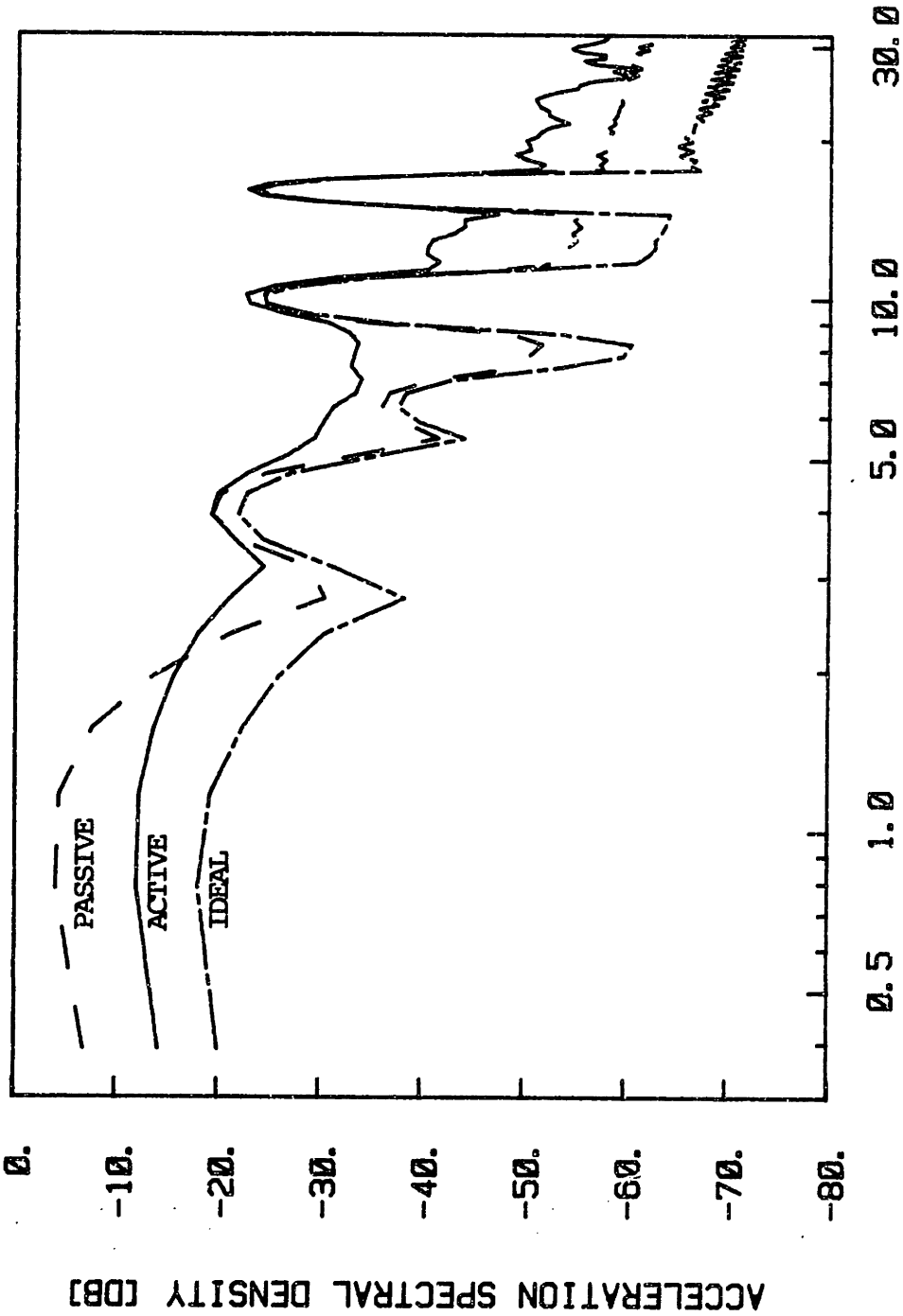

FIGURE 4.2.7 ACCELERATION POWER SPECTRAL DENSITY OF PASSIVE, ACTIVE AND IDEAL SYSTEMS.

valve orifice area, and the opening and closing pure time delays of the valve, are fixed parameters that only depend on the actuator and valve chosen. Although all the above parameters affect the performance of the system, the latter set, determines the physical and economical system's limitations, and special care should be taken in their selection. Throughout this section, the first set of parameters, which only affect the controller, will be referred to as "tuning parameters", while the others, which directly depend on the valve/actuator characteristics, will be referred to as "fixed parameters".

The relative effect of changing each of the "fixed parameters" was studied by choosing the "tuning parameters" so that the best acceleration performance could be achieved. Even though the nonlinearities present in the system make it very difficult to evaluate the performance of the system when changing more than one parameter at the same time, the results obtained served to give some insight into the behavior of the system, which could be used when designing nonlinear active pneumatic suspension systems.

The effect of changing the actuator diameter, while keeping all the other "fixed parameters" constant, was evaluated first. Figure 4.3.1 shows the r.m.s. carbody lateral acceleration, the r.m.s. carbody stroke and the average air flow consumption per truck as obtained by using

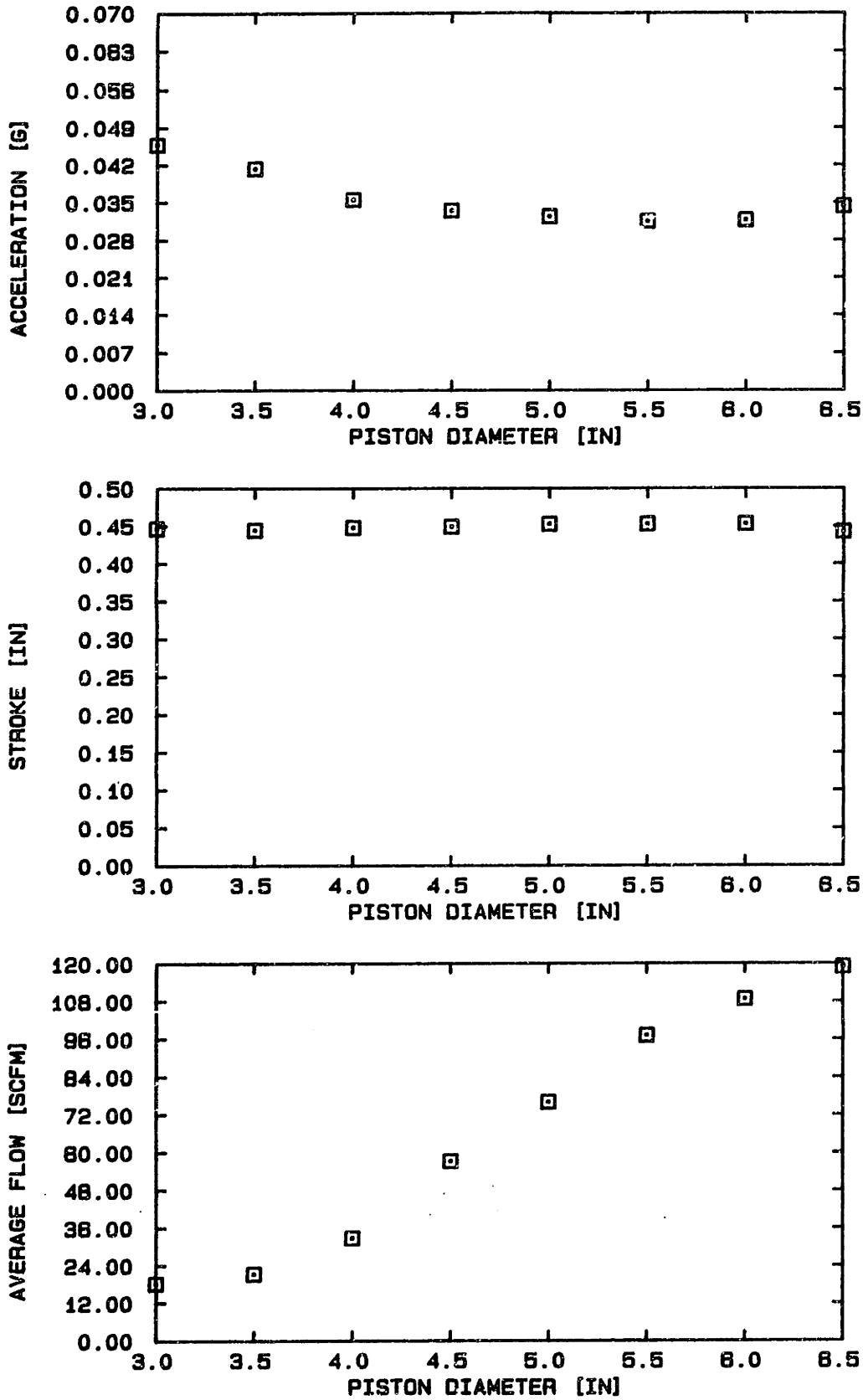

FIGURE 4.3.1 ACTIVE SUSPENSION PERFORMANCE AS A FUNCTION OF ACTUATOR DIAMETER.

the subroutine SYS. As the actuator diameter is increased, the r.m.s. carbody acceleration is decreased to a minimum value, and then it is increased again. For a given supply pressure, the peak force that the actuator is able to apply, and therefore its ability to reduce lateral acceleration, is increased with the actuator diameter. However, since the volume of the actuator is also increased, its bandwidth is reduced. This augments the system lag, causing a rise in the r.m.s. carbody acceleration obtained for actuator diameters larger than 5.5 inches. The r.m.s. stroke remains constant as the actuator diameter is changed. The average flow consumption, however, experiences a continuous rise as the actuator diameter is increased. This is also due to the larger actuator volume. As the actuator volume is increased, the amount of work needed to compress the air inside the actuator is also increased, increasing the power consumption.

Figure 4.3.2 shows the system performance as a function of the effective orifice area of the valve. The r.m.s. carbody acceleration, and the r.m.s. stroke remain constant as the effective orifice area of the valve is increased. This was attributed to the controller's ability to regulate the force produced by the actuator, despite the air flow passing through the valve. Since the closing pure time delay was kept constant, the amount of air that was going in and out of the actuator was larger, therefore producing a continuous increase of the average air flow consumption.

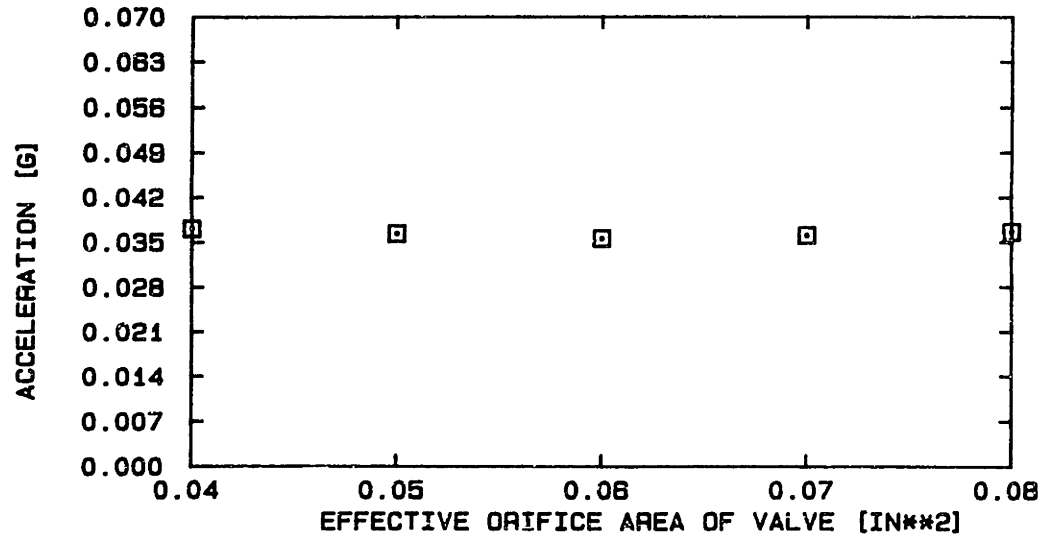

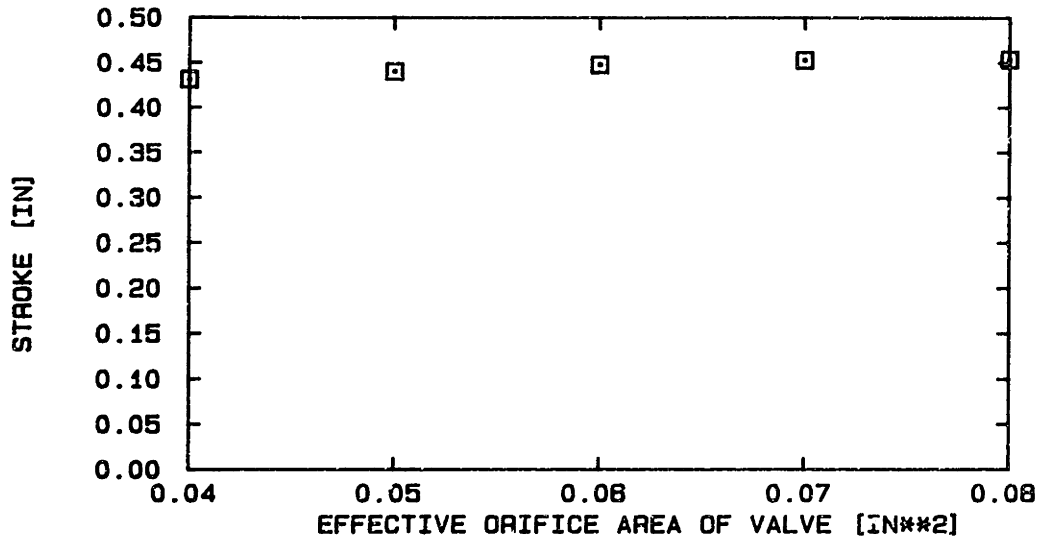

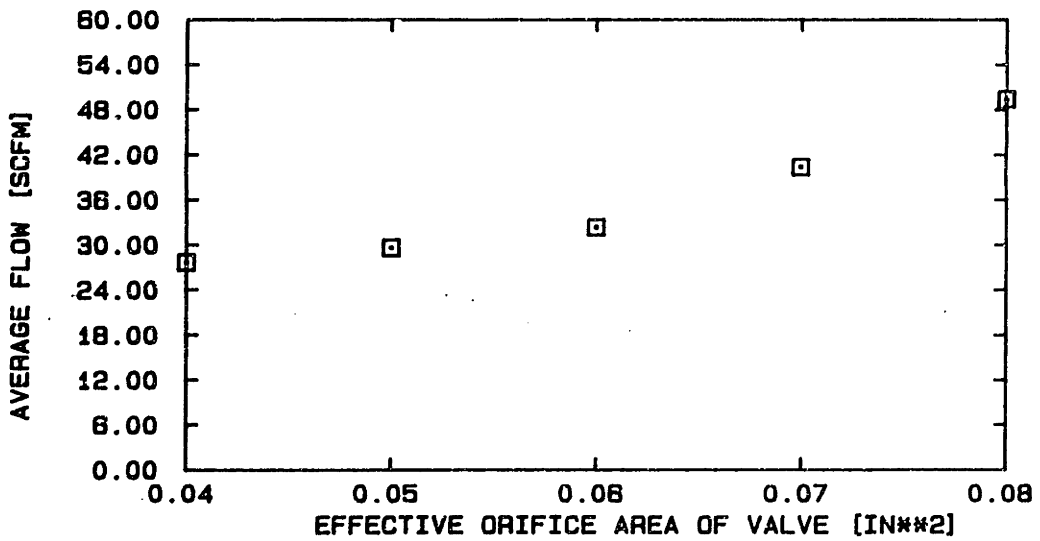

FIGURE 4.3.2 ACTIVE SUSPENSION PERFORMANCE AS A FUNCTION OF ORIFICE AREA OF THE VALVE.

Figure 4.3.3 shows the influence of changing the opening time delay of the valve on the system response. As the opening time delay is increased, the bandwidth of the system is reduced. This increases the "overall stiffness" of the system, producing an increase in the r.m.s. carbody acceleration, and a decrease in the r.m.s. carbody stroke. Larger opening time delays also reduce the average time that both the input and output valves are open, causing a reduction in the average air flow consumption.

As the close pure time delay is increased, the r.m.s. acceleration is slightly increased, while the r.m.s. stroke is reduced. This, again, is due to a decrease in the system bandwidth. Since a larger time is required to close the valves, the average air flow going in and out of the actuators is increased, producing a continuous rise of the power consumption. Fig. 4.3.4, shows how the system performance changes as a function of the closing time delay.

Figures 4.3.1 to 4.3.4 suggest that 4 inch bore pneumatic cylinders and solenoid valves having an opening time delay of 50 ms, an effective orifice area of 0.04 square inches and a closing time delay of 25 ms or less are a good choice of the active suspension "fixed parameters". With these valves and actuators a 48% reduction in the r.m.s. carbody lateral acceleration could be achieved while requiring only 7-9.7 horsepower/car. Larger actuators could be used to

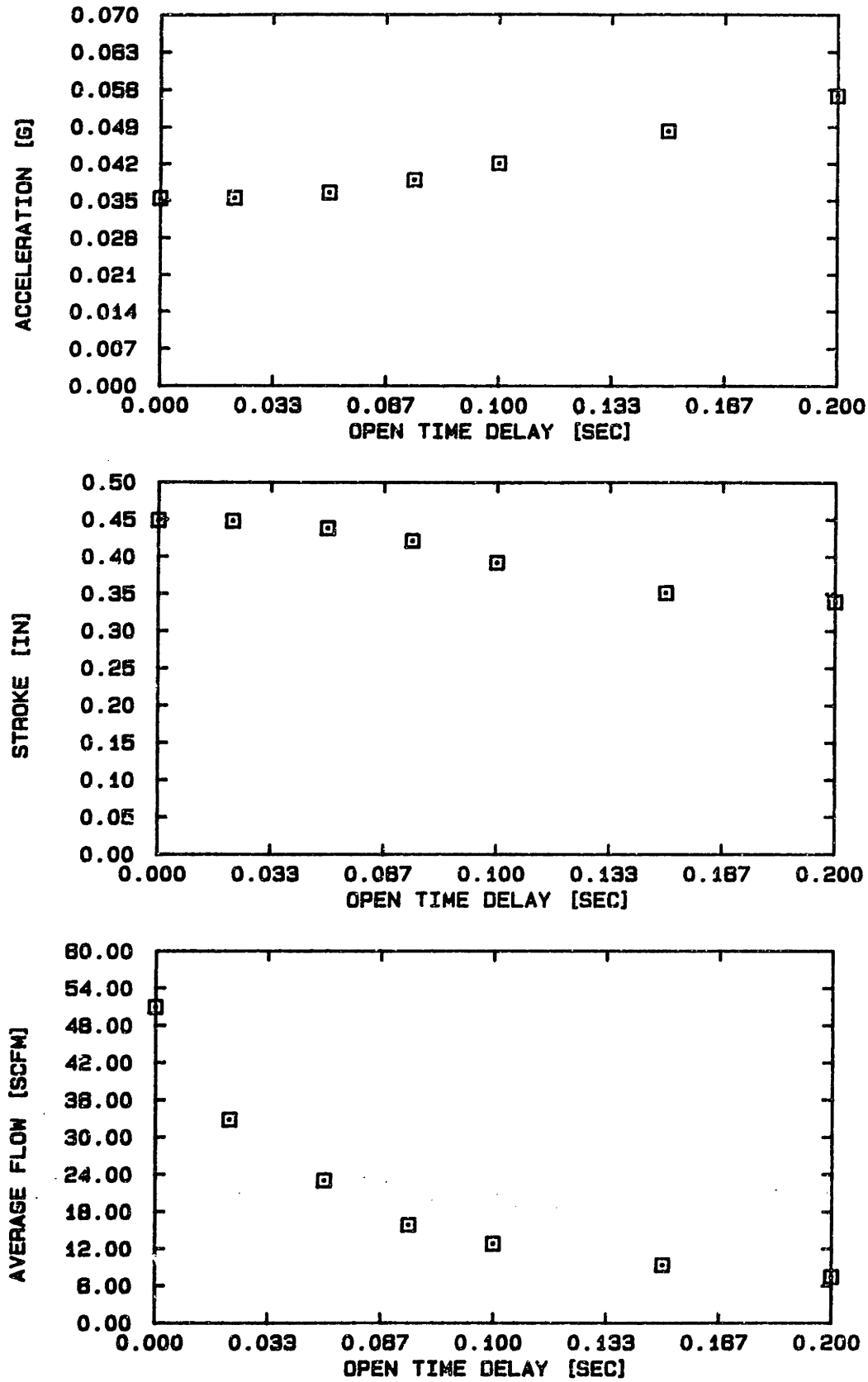

FIGURE 4.3.3 ACTIVE SUSPENSION PERFORMANCE AS A FUNCTION OF OPENING TIME DELAY OF THE VALVE.

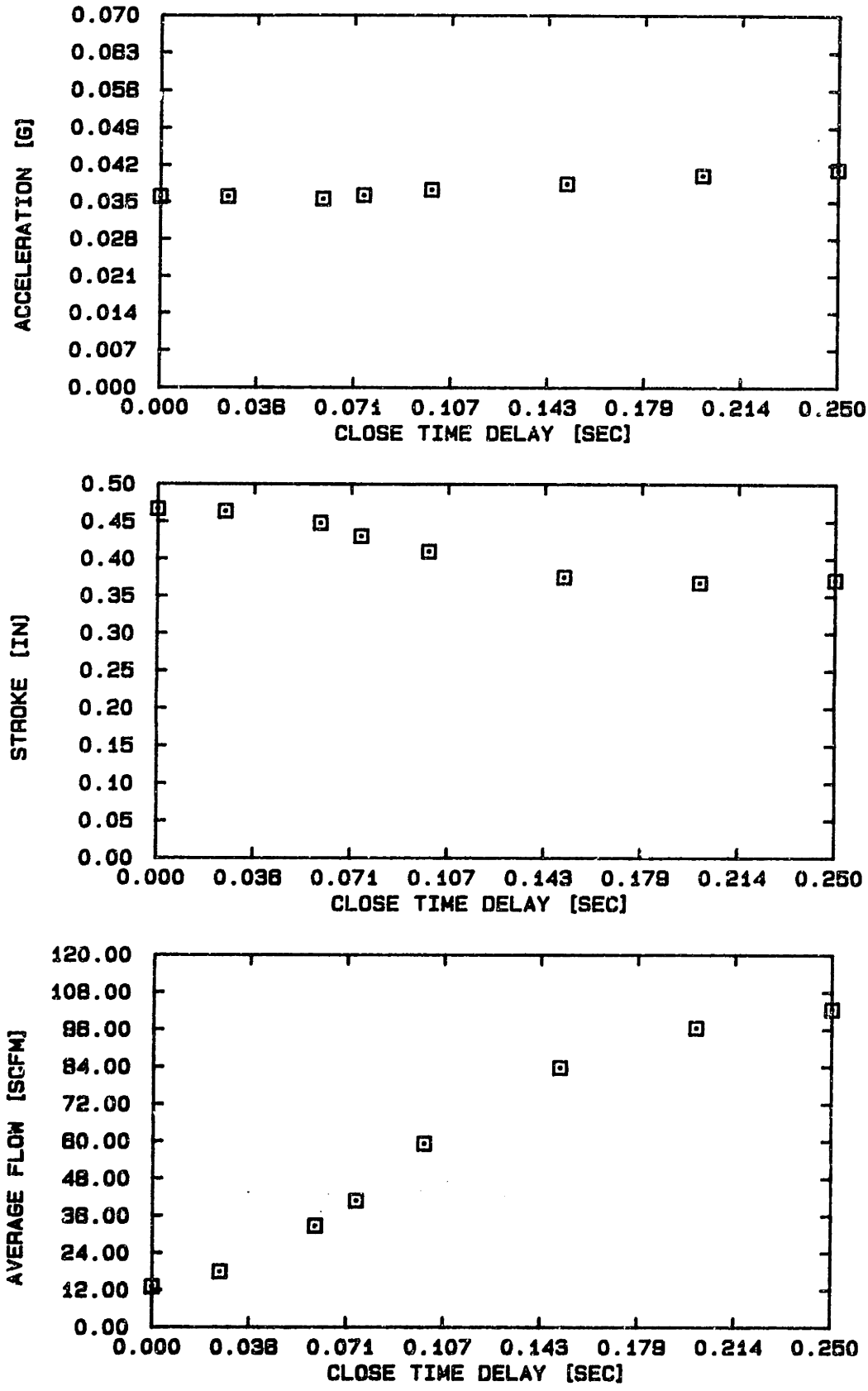

FIGURE 4.3.4 ACTIVE SUSPENSION PERFORMANCE AS A FUNCTION OF CLOSING TIME DELAY OF THE VALVE.

slightly improve acceleration reductions, but at the expense of significantly increasing the air flow consumption. Smaller actuators, on the other hand, could be used to reduce the air flow consumption, but at the expense of largerly degrading the acceleration response. Smaller opening time delays would increase the air flow consumption, while larger opening time delays would degrade the system response. Valves having a larger orifice area would increase the air flow consumption without improving the acceleration performance. Smaller closing time delays would reduce the system air flow consumption, while improving acceleration performance. However, valves having small time delays would be more and dificult to find.

The existing onboard compressor on Amtrak's F-40 diesel locomotive is capable of providing 130 horsepower at a nominal pressure of 130 psig. This compressor, however, can only be operated at 20-30% of full capacity so that sufficient time to filter and cool the air leaving the compressor is allowed and overheating does not occur [14]. With these limitations, a maximun of 39 horsepower could be used to operate the active suspension system. For a ten passenger car train this gives a maximun average air flow rate of 9.36 scfm/truck. To reduce the active suspension air flow to this value, valves having an opening time delay of 150 ms, an effective orifice area of 0.06 square inches and a closing time delay of 60 ms could be used. If these valves and 4 inch

bore pneumatic cylinders were used, the r.m.s. carbody lateral acceleration could be reduced by 30% to 0.049g while satisfying the power consumption limitations. To achieve better acceleration performance a larger compressor would be required.

The parametric studies have shown that a trade off exists between the r.m.s. acceleration reduction, the initial installation costs, and the average power consumption. This trade off problem must be resolved if a pneumatic active suspension is to be designed. Therefore, the final selection of the system components will depend on the design specifications and on the designer's financial restrictions.

Chapter 5

SEMI-ACTIVE SUSPENSIONS

5.1 INTRODUCTION

Although the nonlinear active suspension proposed in this thesis was shown to perform well when applied to improve the ride quality performance of rail vehicles, the need for an external power supply makes its implementation costly if the already existing onboard compressor can not be utilized. As an alternative to improve ride quality performance, while reducing the installation and the operation costs, the feasibility of using a semi-active vibration isolator was considered.

Semi-active suspension systems, are in general, externally controllable force generators, where the force is developed by the relative velocity of its attachment points. By controlling the damping characteristics of a viscous damper, a controllable force related to any state or combination of states can be applied to the system. Since external power is only used for signal processing and valve

actuation, and not for applying energy into the system, a very low power is required.

In semi-active suspensions systems, forces can only be produced when the power associated with such forces is dissipated. For this reason, during portion of its operation, when the command force and the available force are in opposite directions, the semi-active suspension is controlled to produce zero force. Although this condition degrades system performance relative to a fully active system, it has been shown [20] that improved performance over passive suspensions can be achieved.

Although semi-active suspensions are always nonlinear, and in general, microprocessor control is required to implement the control law, its implementation is less expensive than that of a fully active suspension system. In this chapter, the performance of an ideal semi-active suspension is investigated analytically using computer simulation and compared to that of passive and fully active systems.

5.2 THE CONTROL LAW

Semi-active suspension systems are usually implemented by using active dampers connected in parallel with passive

springs. The active damper is essentially a passive device capable of externally controlling the force across the damper independently of the relative velocity of its attachment points. The damping coefficient and, therefore, the damping force are controlled by modulation of the damper orifice. In this study, an infinite bandwidth of the orifice modulating device was assumed, and therefore the characteristics of an ideal semi-active suspension system were evaluated.

The control strategy used, was to modulate the passively generated damper force to equal the force that would be generated by a damper connected between the carbody and some inertial reference ("skyhook damper", Fig. 2.2.2). This was achieved by using the control law:

$$Fd = -K1\ \dot{Y}c \qquad (5.2.1)$$

where Fd is the desired force across the active damper, $\dot{Y}c$ is the absolute carbody velocity, and K1 is the velocity feedback gain.

Since no external power is supplied to the active damper system, this force can only dissipate power; therefore, the device will be capable of applying this force if and only if:

$$\dot{Y}c(\dot{Y}c-\dot{Y}t) > 0 \qquad (5.2.2)$$

where $\dot{Y}c$ is the absolute truck velocity. When $\dot{Y}c$ and $(\dot{Y}c-\dot{Y}t)$

are of opposite sign, the active damper can only supply a force opposite to the desired force Fd. In this case, the best the active damper can do to approximate the desired force is to apply no force at all. When $(\dot{Y}c-\dot{Y}t)$ is equal to zero, the active damper responds by attempting to generate the desired force Fd. If the desired force is larger that the maximum available damper force, the active damper will lock up the system producing a force:

$$Fa = M\,\ddot{Y}c + K(Yc-Yt) \qquad (5.2.3)$$

The control force applied by the active damper, Fa, will then have three different possible values:

$$Fa = Fd \text{ if } \dot{Y}c(\dot{Y}c-\dot{Y}t) > 0 \qquad (5.2.4)$$

$$Fa = 0 \text{ if } \dot{Y}c(\dot{Y}c-\dot{Y}t) < 0 \qquad (5.2.5)$$

$$Fa = M\,\ddot{Y}c + K(Yc-Yt) \text{ if } \dot{Y}c-\dot{Y}t = 0 \qquad (5.2.6)$$

The device will switch among these three possibles values, producing a control force which is obviously nonlinear.

5.3 PERFORMANCE OF SEMI-ACTIVE SUSPENSIONS

In order to evaluate the characteristics of an ideal semi-active suspension system when applied to improve the ride quality performance of rail vehicles the FORTRAN subroutine SEMI (appendix 3) was utilized. In this subroutine the

carbody lateral dynamics was simulated by using the one degree of freedom model developed in chapter two. The baseline parameters of an Amtrak passenger-coach train with zero lateral secondary suspension damping coefficient, and the pseudo-random disturbance input modeled by Cho [13], were used as an example for this study.

Fig. 5.3.1 and 5.3.2 show the acceleration power spectral density of the semi-active system as compared to the passive case for different values of the velocity feedback gain, K1. As the velocity feedback gain is increased, the low frequency acceleration attenuation is also increased, at the expense of an amplification of the high frequency acceleration response. This trade off between the low and high frequency acceleration attenuation, was attributed to the power limitations inherent to the active damper system. As the velocity feedback gain is increased, the sensitivity of the system to switch among the possible force values is increased. This produces a high frequency actuator force that, although capable of reducing low frequency accelerations, increases the high frequency acceleration response of the system.

Table 5.1 shows the r.m.s. carbody lateral acceleration, the r.m.s. suspension stroke and their percentage of reduction as compared to the passive case. When the velocity feedback gain, K1, is increased the r.m.s.

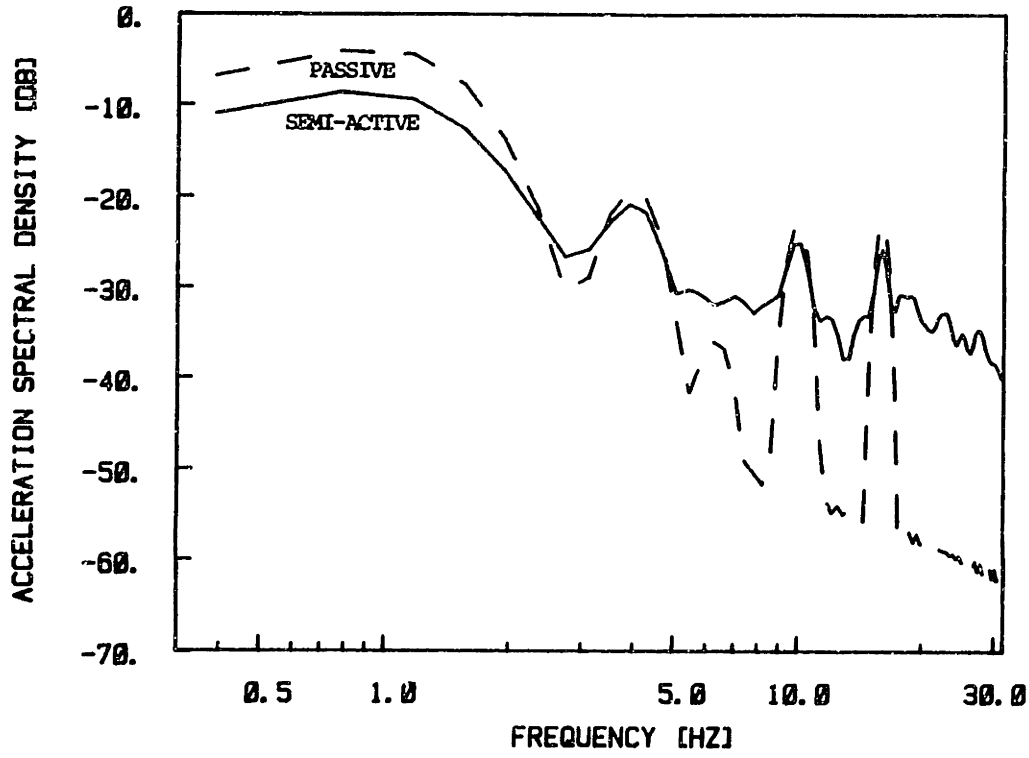

K1 = 500 lbf-sec/in

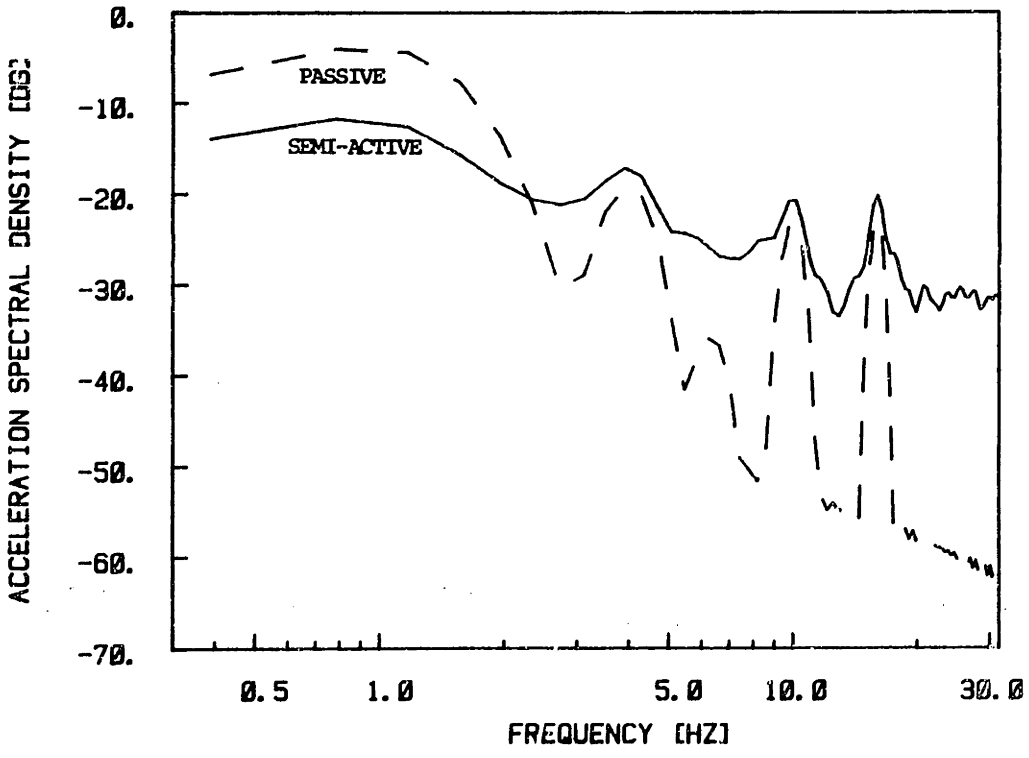

K1 = 1000 lbf-sec/in

FIGURE 5.3.1 SEMI-ACTIVE SYSTEM ACCELERATION POWER SPECTRAL DENSITY FOR VELOCITY FEEDBACK GAINS OF 500 AND 1000 LBF-SEC/IN.

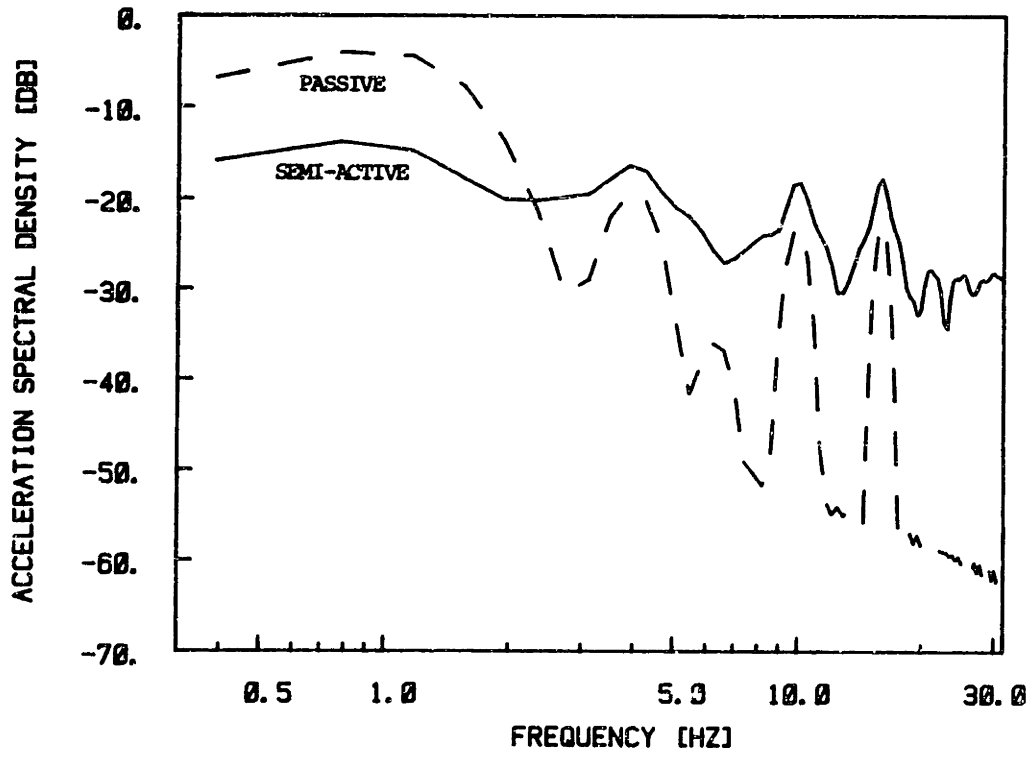

K1 = 1500 lbf-sec/in

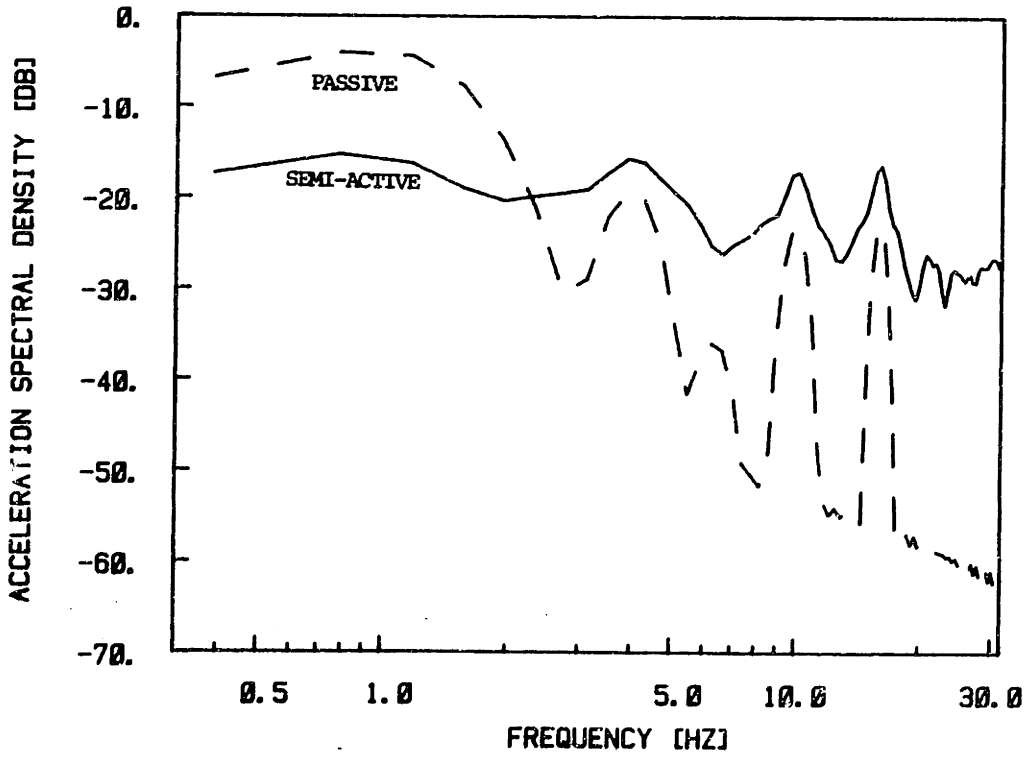

K1 = 2000 lbf-sec/in

FIGURE 5.3.2 SEMI-ACTIVE SYSTEM ACCELERATION POWER SPECTRAL DENSITY FOR VELOCITY FEEDBACK GAINS OF 1500 AND 2000 LBF-SEC/IN.

A	B	C	D	E
500	0.046	0.49	34	23
1000	0.041	0.45	41	30
1500	0.043	0.44	37	31
2000	0.045	0.45	36	30

A = Velocity feedback gain, lbf-sec/in;

B = R.M.S carbody acceleration, g;

C = R.M.S. secondary suspension travel, in;

D = R.M.S acceleration change from passive, %;

E = R.M.S secondary suspension travel change from passive, %.

Table 5.1.- SEMI-ACTIVE SUSPENSION PERFORMANCE

lateral carbody acceleration is reduced to a minimum, and then it is increased again. In this study, the value of K1 that minimizes the r.m.s. lateral carbody acceleration was used to evaluate the effectiveness of the ideal semi-active suspension system.

Figure 5.3.3 shows the carbody lateral acceleration as a function of time when a velocity feedback gain of 1000 lbf-sec/in is used. For this case, the peak lateral carbody acceleration was reduced by 47% to 0.090g, and the r.m.s. lateral carbody acceleration was reduced by 41% to 0.041g. Figure 5.3.4 shows the active damper force Fa as compared to the desired force Fd. As it can be seen, the power limitations inherent to the active damper system produces a high frequency oscillation in the actuator force. These high frequency oscillations are especially increased when the difference between the carbody and truck velocity is near to zero. When the relative velocity is driven through zero, the applied force drops to zero. If the relative velocity is again passed through zero, the actuator force begins to built up trying to drive the relative velocity through zero again, and so on. This produces a limited cycling oscillation which is eventually broken out when the variables Yc and Yt are changed by a significan amount.

Figure 5.3.5 shows a comparison of the acceleration power spectral density of the carbody when using the ideal

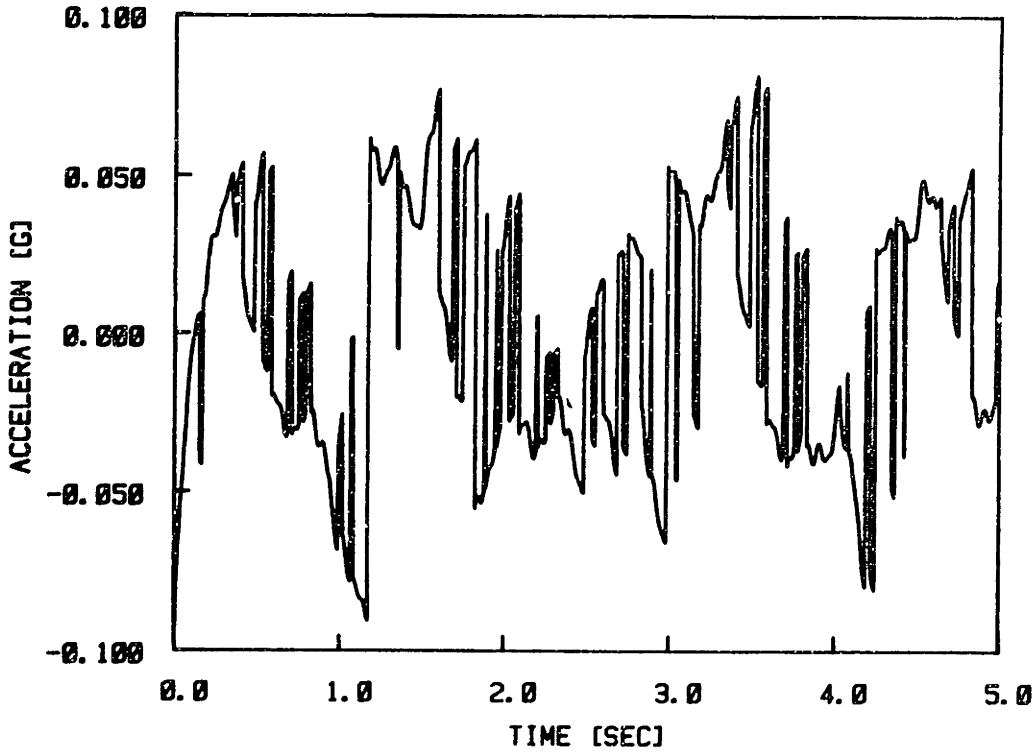

FIGURE 5.3.3 SEMI-ACTIVE SYSTEM ACCELERATION RESPONSE.

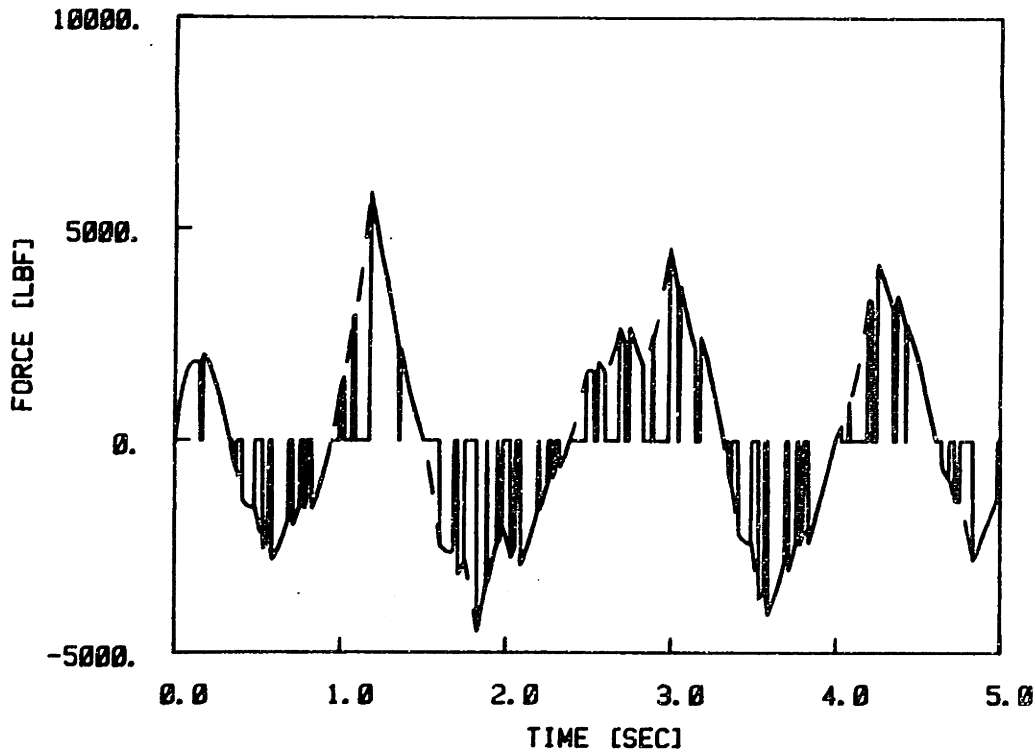

FIGURE 5.3.4 SEMI-ACTIVE SYSTEM DESIRED AND ACTUAL ACTUATOR FORCE.

semi-active suspension, the ideal fully active suspension and the nonlinear active pneumatic suspension proposed in this thesis. For frequencies below 2.5 hz, the ideal semi-active suspension and the nonlinear active pneumatic suspension are capable of providing similar improvement in acceleration performance. At higher frequencies, however, the performance limits of the semi-active suspension are apparent when compared to the nonlineal active pneumatic system. The ideal semi-active system is capable of providing 82% of the r.m.s. carbody lateral acceleration reduction possible using pneumatic active suspensions and 55% of the reduction predicted for the ideal active suspension system.

In a real semi-active suspension device, the limited bandwidth of the valve used to modulated the force across the active damper introduces a lag in the actuator response. Also, the minimum force that the active damper can apply is limited by the maximum orifice opening of the valve. It has been shown [20] that these implementation limitations degrade the simi-active suspension's capability of improving acceleration performance, even for low frequencies disturbances.

Although a quantitative evaluation of the performance improvement that can be achieved using real active dampers is required, it is clear that active suspension system are capable of improving ride quality performance beyond the

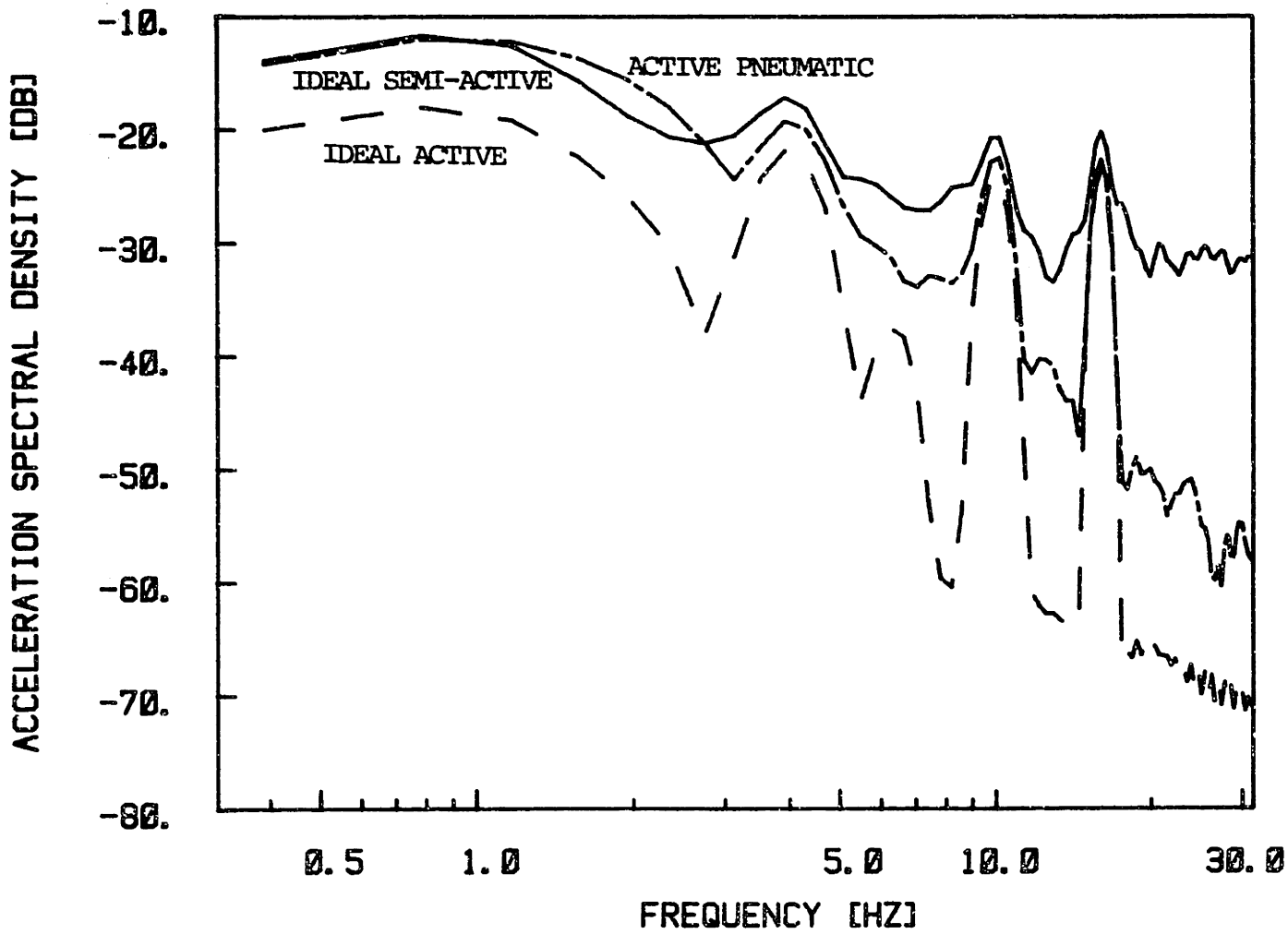

FIGURE 5.3.5 ACCELERATION POWER SPECTRAL DENSITY OF SEMI-ACTIVE, ACTIVE PNEUMATIC AND IDEAL ACTIVE SYSTEMS.

Appendix 2

ROUTINE SYS

```
C                       SUBROUTINE SYS.
C
C     This  subroutine  is  run  with a fourth order Runge-Kutta
C     routine and evaluates the  performace  of active pneumatic
C     suspensions  subject  to a  random disturbance.
C
C
      SUBROUTINE DIFEQ
      COMMON  T,DT,Y(30),F(30),STIME,FTIME,DTNEW,N
      REAL    Mc,Ksy,Kbump
      REAL    k
      REAL    kd(2),Yti(9),Freq(9),Phs(9),Wf(9)
      EQUIVALENCE (Y(1),Yc),(Y(2),Vc),(Y(3),Pa),(Y(4),Pb)
C
C     DTNEW is set as follows:
C           DTNEW =  0, on first call of DIFEQ,
C           DTNEW =  1, at intermediate integration steps,
C           DTNEW = -1, at the begining of an integration step.
C
      IF (DTNEW .NE. 0.) GO TO 20
C
C     Reading of system parameters.
C
      OPEN(10,FILE='OUT')
      OPEN(8,FILE='DAT')

      READ(8,*) NDUM
      READ(8,*) Mc,Ksy,Kbump,Csy

      READ(8,*) NDUM
      READ(8,*) Vo,Apo

      READ(8,*) NDUM
      READ(8,*) Kd(1),Kd(2)

      READ(8,*) NDUM
      READ(8,*) k,R,Ts,g,Ro

      READ(8,*) NDUM
      READ(8,*) Pe,Ps,Amax,On,Off,Err,Dlead

      READ(8,*) NDUM
      READ(8,*) (Yti(I),I=1,9)

      READ(8,*) NDUM
      READ(8,*) (Freq(I),I=1,9)

      READ(8,*) NDUM
      READ(8,*) (Phs(I),I=1,9)
```

```
      CLOSE(8)
C
C     Variable initialization.
C
      Yc   =   0.0
      Vc   =   0.0
      Pa   =   Pe
      Pb   =   Pe

      DO 15 I=1,9
15        Wf(I)   =   2.*3.14*Freq(I)

      Count    =   0.0
      SumYc    =   0.0
      SumYc2   =   0.0
      SumVact  =   0.0
      SumVact2=    0.0
      SumYt    =   0.0
      SumYt2   =   0.0
      SumFrc   =   0.0
      SumFrc2  =   0.0
      SumAc    =   0.0
      SumAc2   =   0.0
      SumStr   =   0.0
      SumStr2  =   0.0
      SumW     =   0.0
      SumW2    =   0.0
C
C     This section is executed only at each new time step.
C
20    IF (DTNEW .EQ. 1) GO TO 10
C
C     Calculation of carbody acceleration.
C
      Stroke   =   Yt -Yc
      Vact     =   Vt -Vc

      Fbump    =   0.0
      IF (Stroke .GT. 1.5) Fbump = Kbump*(Stroke-1.5)
      IF (Stroke .LT.-1.5) Fbump = Kbump*(Stroke+1.5)
      Accel    =   (Ksy*Stroke+Fbump+Csy*Vact+Force)/Mc
      Acc      =   Accel/g
C
C     Calculation of actual actuator force.
C
      Force0   =   Force
      Force    =   Pa*Apo - Pb*Apo
C
C     Calculation of desired force.
C
```

```
      Fvel     =   Kd(1) * Vc
      Faccel   =   Kd(2) *Accel
      Fi0      =   Fi
      Fi       =   Fvel + Faccel
C
C     Lead compensation of the error.
C
      Ferror   =   (Fi-Force)+Dlead*((Fi-Fi0)/DT
      1             -(Force-Force0/DT)
C
C     Calculation of controller voltage output.
C
      IF (ABS(Ferror) .LE. Err) THEN
          V1   =   0.0
          V2   =   0.0
          V3   =   0.0
          V4   =   0.0
          GO TO 60
      ENDIF
      IF (Ferror .GT. 0.0) THEN
          V1   =   24.0
          V2   =   0.0
          V3   =   24.0
          V4   =   0.0
          GO TO 60
      ELSE
          V1   =   0.0
          V2   =   24.0
          V3   =   0.0
          V4   =   24.0
          GO TO 60
      ENDIF
C
C     Computation of valve dynamics.
C
60    CALL VALVE(V1,V10,D1,Ae1,Tf1,DT,On,Off,T,Amax,F31)
      CALL VALVE(V2,V20,D2,Ae2,Tf2,DT,On,Off,T,Amax,F32)
      CALL VALVE(V3,V30,D3,Ae3,Tf3,DT,On,Off,T,Amax,F33)
      CALL VALVE(V4,V40,D4,Ae4,Tf4,DT,On,Off,T,Amax,F34)
C
C     Computation of averages and variances.
C
      W1c          =   W1*60./Ro
      W4c          =   W4*60./Ro

      Count        =   Count   +   1
      SumYc        =   SumYc   +   Yc
      SumYc2       =   SumYc2  +   Yc**2
      SumYt        =   SumYt   +   Yt
      SumYt2       =   SumYt2  +   Yt**2
```

```
      SumVact      =   SumVact +   Vact
      SumVact2     =   SumVact2+   Vact**2
      SumFrc       =   SumFrc  +   Force
      SumFrc2      =   SumFrc2 +   Force**2
      SumAc        =   SumAc   +   Acc
      SumAc2       =   SumAc2  +   Acc**2
      SumStr       =   SumStr  +   Stroke
      SumStr2      =   SumStr2 +   Stroke**2
      SumW         =   SumW    +   W1c+W4c
      SumW2        =   SumW2   +   (W1c+W4c)**2

      IF (T .GE. FTIME) THEN

          AYc      =   SumYc/Count
          VYc      =   ((SumYc2-SumYc**2/Count)/(Count-1))
          SVYc     =   SQRT(VYc)
          AYt      =   SumYt/Count
          VYt      =   ((SumYt2-SumYt**2/Count)/(Count-1))
          SVYt     =   SQRT(VYt)
          AVact    =   SumVact/Count
          VVact    =   ((SumVact2-SumVact**2/Count)/(Count-1))
          SVVact   =   SQRT(VVact)
          AFrc     =   SumFrc/Count
          VFrc     =   ((SumFrc2-SumFrc**2/Count)/(Count-1))
          SVFrc    =   SQRT(VFrc)
          AAc      =   SumAc/Count
          VAc      =   ((SumAc2-SumAc**2/Count)/(Count-1))
          SVAc     =   SQRT(VAc)
          AStr     =   SumStr/Count
          VStr     =   ((SumStr2-SumStr**2/Count)/(Count-1))
          SVStr    =   SQRT(VStr)
          AW       =   SumW/Count
          VW       =   ((SumW2-SumW**2/Count)/(Count-1))
          SVW      =   SQRT(VW)
C
C     Writing  of  the  computed  averages  and variances to an
C     external file and console.
C
          WRITE(1,70)
          WRITE(10,70)
          WRITE(1,71) AYc,SVYc
          WRITE(10,71) AYc,SVYc
          WRITE(1,72) AYt,SVYt
          WRITE(10,72) AYt,SVYt
          WRITE(1,73) AVact,SVVact
          WRITE(10,73) AVact,SVVact
          WRITE(1,74) AFrc,SVFrc
          WRITE(10,74) AFrc,SVFrc
          WRITE(1,75) AAc,SVAc
          WRITE(10,75) AAc,SVAc
```

```
            WRITE(1,76) AStr,SVStr
            WRITE(10,76) AStr,SVStr
            WRITE(1,77) AW,SVW
            WRITE(10,77) AW,SVW

            CLOSE(10)

70          FORMAT(//25X,'Mean',14X,'Desviation'//)
71          FORMAT(1X,'Yc',15X,F10.4,11X,F10.4/)
72          FORMAT(1X,'Yt',15X,F10.4,11X,F10.4/)
73          FORMAT(1X,'Vact',13X,F10.4,11X,F10.4/)
74          FORMAT(1X,'Force',12X,F10.2,11X,F10.2/)
75          FORMAT(1X,'Accel',12X,F10.4,11X,F10.4/)
76          FORMAT(1X,'Stroke',11X,F10.4,11X,F10.4/)
77          FORMAT(1X,'Flow',13X,F10.4,11X,F10.4/)

         ENDIF
C
C     This section is run four times for each time step.
C
C     Computation of disturbance input.
C
10       Yt  =   0.0
         Vt  =   0.0
         DO 25 I=1,9
            Yt  =   Yt - ( Yti(I) * SIN (Wf(I)*T+Phs(I)))
25          Vt  =   Vt - ( Wf(I) * Yti(I) * COS (Wf(I)*T+Phs(I)))
C
C     Calculation of adiabatic temperatures.
C
         Ta  =   (Pa/Ps)**(1.-1./k)*Ts
         Tb  =   (Pb/Ps)**(1.-1./k)*Ts

         CALL FLOW (Pa,Ps,Ae1,Ts,W1)
         CALL FLOW (Pe,Pa,Ae2,Ta,W2)
         CALL FLOW (Pe,Pb,Ae3,Tb,W3)
         CALL FLOW (Pb,Ps,Ae4,Ts,W4)
C
C     Calculation of actuator capacitance.
C
         Wa  =   W1 - W2
         Wb  =   W4 - W3

         Va  =   Vo - (YT-YC)*Apo
         Vb  =   Vo + (YT-YC)*Apo

         Cva =   Va*g/(k*R*Ta)
         Cvb =   Vb*g/(k*R*Tb)
```

Page 6 of program SYS

```
C
C     System's differential equations.
C
      F(1)     =    Vc

      Fbump    =    0.0
      IF ((Yt-Yc) .GT. 1.5) Fbump = (Yt-Yc+1.5)*Kbump
      IF ((Yt-Yc) .LT.-1.5) Fbump = (Yt-Yc-1.5)*Kbump
      F(2)     =    (Ksy*(Yt-Yc)+Fbump+Csy*(Vt-Vc)
      1             +(Pa*Apo-Pb*Apo))/Mc

      F(3)     =    Wa/Cva-k*Pa*Apo*(Vc-Vt)/Va

      F(4)     =    Wb/Cvb+k*Pb*Apo*(Vc-Vt)/Vb

      RETURN
      END
```

```
C
C                        SUBROUTINE VALVE
C
C     This subroutine  calculates the dynamics  of the valve by
C     the simulation of the opening and closing time delays.
C
      SUBROUTINE VALVE(V,V0,Dp,Ae,Tf,DT,On,Off,T,Amax,F3)
      IF (V .EQ. V0) GO TO 20
      Dp  =   0.0
      F3  =   0.0
20    V0  =   V
      IF (V.EQ. 24.) THEN
          Tdp =   On/DT
          Dp  =   Dp + 1.
          IF (Dp .LT. Tdp) RETURN
          IF (F3 .EQ. 0.0) Tf=T
          F3  =   1.
          Ae  =   Amax
          RETURN
         ELSE
          Tdp =   Off/DT
          Dp  =   Dp + 1.
          IF (Dp .LT. Tdp) RETURN
          IF (F3 .EQ. 0.0) Tf=T
          F3  =   1.
          Ae  =   0.0
          RETURN
      ENDIF
      END
```

```
C                          SUBROUTINE FLOW
C
C     This subroutine calculates  the compressible  flow through
C     a valve.
C
      SUBROUTINE FLOW(Pd,Pu,Aeff,Ts,W)
      REAL K
      C1   =    2.06
      C2   =    0.532
      k    =    1.4

      IF (Pd/Pu .LE. 0.528) GO TO 10
      IF (Pd .GT. Pu) GO TO 15

      W    =    Aeff*C1*Pu/Ts**0.5*(Pd/Pu)**(1./k)*(1.-(Pd/Pu)**
     1          ((k-1.)/k))**0.5
      RETURN

15    Pue  =    Pd
      Pde  =    Pu
      W    =    -Aeff*C1*Pue/Ts**0.5*(Pde/Pue)**(1./k)
     1          *(1.-(Pde/Pue)**((k-1.)/k))**0.5
      RETURN

10    W    =    Aeff*C2*Pu/Ts**0.5
      RETURN
      END
```

Appendix 3

ROUTINE SEMI

```
C                       SUBROUTINE SEMI
C
C     This  subroutine  is  run  with a fourth order Runge-Kutta
C     routine  and  evaluates the  performace  of an ideal semi-
C     active suspensions  subject  to a  random disturbance.
C
C
      SUBROUTINE DIFEQ
      COMMON  T,DT,Y(30),F(30),STIME,FTIME,DTNEW,N
      REAL    Mc,Ksy,Kbump
      REAL    kd,Yti(9),Freq(9),Phs(9),Wf(9)
      EQUIVALENCE (Y(1),Yc),(Y(2),Vc)
C
C     DTNEW is set as follows:
C           DTNEW =  0, on first call of DIFEQ,
C           DTNEW =  1, at intermediate integration steps,
C           DTNEW = -1, at the begining of an integration step.
C
      IF (DTNEW .NE. 0.) GO TO 20
C
C     Reading of system parameters.
C
      OPEN(10,FILE='OUT')
      OPEN(8,FILE='DAT')

      READ(8,*) NDUM
      READ(8,*) Mc,Ksy,Kbump

      READ(8,*) NDUM
      READ(8,*) Kd

      READ(8,*) NDUM
      READ(8,*) g

      READ(8,*) NDUM
      READ(8,*) Pe

      READ(8,*) NDUM
      READ(8,*) (Yti(I),I=1,9)

      READ(8,*) NDUM
      READ(8,*) (Freq(I),I=1,9)

      READ(8,*) NDUM
      READ(8,*) (Phs(I),I=1,9)

      CLOSE(8)
```

Page 2 of program SEMI

```
C
C     Variable initialization.
C
      Yc   =    0.0
      Vc   =    0.0

      DO 15 I=1,9
15        Wf(I)    =    2.*3.14*Freq(I)

      Count    =    0.0
      SumYc    =    0.0
      SumYc2   =    0.0
      SumVact  =    0.0
      SumVact2=     0.0
      SumYt    =    0.0
      SumYt2   =    0.0
      SumFrc   =    0.0
      SumFrc2  =    0.0
      SumAc    =    0.0
      SumAc2   =    0.0
      SumStr   =    0.0
      SumStr2  =    0.0
C
C     This section is executed only at each new time step.
C
20    IF (DTNEW .EQ. 1) GO TO 10
C
C     Calculation of carbody acceleration.
C
      Stroke   =    Yt -Yc
      Vact     =    Vt -Vc

      Fbump    =    0.0
      IF (Stroke .GT. 1.5) Fbump = Kbump*(Stroke-1.5)
      IF (Stroke .LT.-1.5) Fbump = Kbump*(Stroke+1.5)
      Accel    =    (Ksy*Stroke+Fbump+Force)/Mc
      Acc      =    Accel/g
C
C     Computation of averages and variances.
C

      Count        =    Count    +    1
      SumYc        =    SumYc    +    Yc
      SumYc2       =    SumYc2   +    Yc**2
      SumYt        =    SumYt    +    Yt
      SumYt2       =    SumYt2   +    Yt**2
      SumVact      =    SumVact  +    Vact
      SumVact2     =    SumVact2+     Vact**2
      SumFrc       =    SumFrc   +    Force
```

```
      SumFrc2     =   SumFrc2 +   Force**2
      SumAc       =   SumAc   +   Acc
      SumAc2      =   SumAc2  +   Acc**2
      SumStr      =   SumStr  +   Stroke
      SumStr2     =   SumStr2 +   Stroke**2

      IF (T .GE. FTIME) THEN

          AYc     =   SumYc/Count
          VYc     =   ((SumYc2-SumYc**2/Count)/(Count-1))
          SVYc    =   SQRT(VYc)
          AYt     =   SumYt/Count
          VYt     =   ((SumYt2-SumYt**2/Count)/(Count-1))
          SVYt    =   SQRT(VYt)
          AVact   =   SumVact/Count
          VVact   =   ((SumVact2-SumVact**2/Count)/(Count-1))
          SVVact  =   SQRT(VVact)
          AFrc    =   SumFrc/Count
          VFrc    =   ((SumFrc2-SumFrc**2/Count)/(Count-1))
          SVFrc   =   SQRT(VFrc)
          AAc     =   SumAc/Count
          VAc     =   ((SumAc2-SumAc**2/Count)/(Count-1))
          SVAc    =   SQRT(VAc)
          AStr    =   SumStr/Count
          VStr    =   ((SumStr2-SumStr**2/Count)/(Count-1))
          SVStr   =   SQRT(VStr)
C
C     Writing  of  the  computed  averages  and variances to an
C     external file and console.
C
          WRITE(1,70)
          WRITE(10,70)
          WRITE(1,71) AYc,SVYc
          WRITE(10,71) AYc,SVYc
          WRITE(1,72) AYt,SVYt
          WRITE(10,72) AYt,SVYt
          WRITE(1,73) AVact,SVVact
          WRITE(10,73) AVact,SVVact
          WRITE(1,74) AFrc,SVFrc
          WRITE(10,74) AFrc,SVFrc
          WRITE(1,75) AAc,SVAc
          WRITE(10,75) AAc,SVAc
          WRITE(1,76) AStr,SVStr
          WRITE(10,76) AStr,SVStr

          CLOSE(10)

70        FORMAT(//25X,'Mean',14X,'Desviation'//)
71        FORMAT(1X,'Yc',15X,F10.4,11X,F10.4/)
```

```
72          FORMAT(1X,'Yt',15X,F10.4,11X,F10.4/)
73          FORMAT(1X,'Vact',13X,F10.4,11X,F10.4/)
74          FORMAT(1X,'Force',12X,F10.2,11X,F10.2/)
75          FORMAT(1X,'Accel',12X,F10.4,11X,F10.4/)
76          FORMAT(1X,'Stroke',11X,F10.4,11X,F10.4/)

        ENDIF
C
C     This section is run four times for each time step.
C
C     Computation of disturbance input.
C
10      Yt  =   0.0
        Vt  =   0.0
        DO 25 I=1,9
           Yt  =   Yt - ( Yti(I) * SIN (Wf(I)*T+Phs(I)))
25         Vt  =   Vt - ( Wf(I) * Yti(I) * COS (Wf(I)*T+Phs(I)))
C
C     Calculation of ideal actuator force
C
        Force   =   -Kd*Vc
        IF (Force .GT. 0.0. .AND. Vc .GT. Vt) Force = 0.
        IF (Force .LT. 0.0. .AND. Vc .LT. Vt) Force = 0.
C
C     System's differential equations.
C
        F(1)    =   Vc

        Fbump   =   0.0
        IF ((Yt-Yc) .GT. 1.5) Fbump = (Yt-Yc+1.5)*Kbump
        IF ((Yt-Yc) .LT.-1.5) Fbump = (Yt-Yc-1.5)*Kbump
        F(2)    =   (Ksy*(Yt-Yc)+Fbump+Force)/Mc

        RETURN
        END
```

Appendix 4

VALVE AND SOLENOID SPECIFICATIONS

Solenoid valve Type MX-...

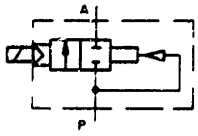

Switching on the voltage excites the solenoid and causes the valve to reverse.

Note: When the pressure is switched on the diaphragm opens briefly.

Caution: When using fluid media, pressure surges may occur during switching.

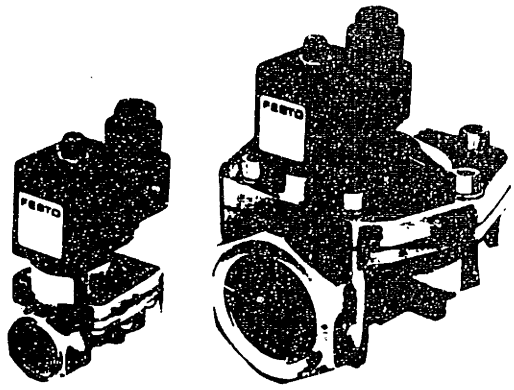

MX-2-⅜ MX-2-1½

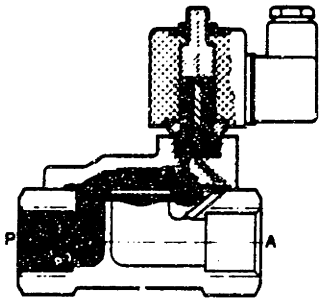

Switching times (according to VDI 3290)

Type	Compressed air ms		Water ms		Oil 22 mm²/s) ms	
	On	Off	On	Off	On	Off
MX-2-¼	20	12	20	35	25	50
MX-2-⅜	20	12	20	35	25	50
MX-2-½	20	12	20	35	25	50
MX-2-¾-B	25	40	25	65	40	70
MX-2-1-B	25	45	25	65	40	70
MX-2-1½	48	65	65	110	75	140

Order designation / Part No./Type	Valve	9601 MX-2-¼	9602 MX-2-⅜	9603 MX-2-½	8646 MX-2-¾-B	8647 MX-2-1-B	9596 MX-2-1½
		+ voltage					
	Mounting bracket	9769 HRM-1			9770 HRM-2		9771 HRM-3
Medium*		Filtered, lubricated or filtered, non-lubricated compressed air, neutral water**, mineral-oil-base hydraulic oil up to 22 mm²/s					
Design		Poppet valve, indirectly actuated, with diaphragm control					
Mounting		Line installation, mounting thread or mounting bracket					
Connection		R ¼	R ⅜	R ½	R ¾	R 1	R 1½
Nominal size		13 mm	13 mm	13 mm	20 mm	25 mm	40 mm
Standard nominal flow rate (P → A)		1500 l/min	2160 l/min	2500 l/min	7500 l/min	9000 l/min	12000 l/min
Kv value for water		27.5 l/min	55 l/min	63 l/min	178 l/min	225 l/min	533 l/min
Pressure range		0.8 to 10 bar					
Min. differential pressure for opening		0.8 bar					
Switching time at 6 bar		See table above					
Ambient temperature		-5 to +40° C (for water 0 to +40° C)					
Temperature of medium		-10 to +60° C					
Materials		Valve body: plastic (POM). Diaphragm: perbunan					
Weight		0.365 kg	0.360 kg	0.355 kg	0.585 kg	0.555 kg	0.930 kg
DC voltage	Standard voltages	12, 24 V					
	Special voltages	6 to 220 V					
AC voltage	Standard voltages	24, 42, 110, 220 V/50 and 60 Hz					
	Special voltages	36 to 360 V/50 Hz, 48 to 240 V/60 Hz					
Power consumption DC voltage		10.8 W					
AC voltage		50 Hz: Hold 19 VA, Pull 28 VA; 60 Hz: Hold 15 VA, Pull 22 VA					
Percentage duty cycle		100%					
Degree of protection		IP 65 (DIN 40 050)					

* Other media on request, ** pH value approx. 7

Solenoid
with connector
as per DIN 43650

DC voltage:

Type MSXG-...

AC voltage:

Type MSXW-...

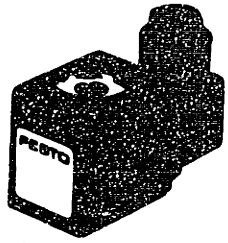

These solenoids are mounted on solenoid valves Type MX and solenoid head Type MKC-032-3.

The complete solenoid head can be mounted on the following valves:
Solenoid valves Type MC, MOC, MLC, JMC,
Type CM-...-C or CH
CJM-...-C or CH
as well as basic valve bodies Type LC, LCO, CLC, CJC, and JLC.

These solenoids are suitable for use under particularly critical operating conditions, for example, where there is relative humidity up to 95% and splashwater.

They correspond to VDE specification 0580 with insulation material of class F. They can be replaced without tampering with the pneumatic circuit.

Test mark: VDE

AC voltage solenoids can be used for 50 and 60 Hz.

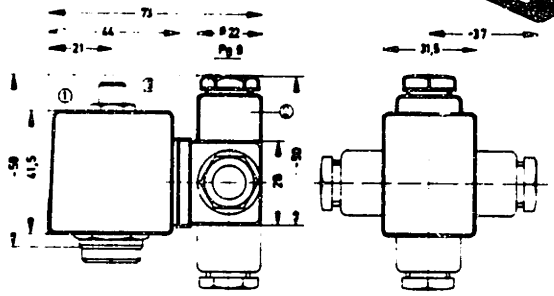

Connector dimensions at 250 to 380 V

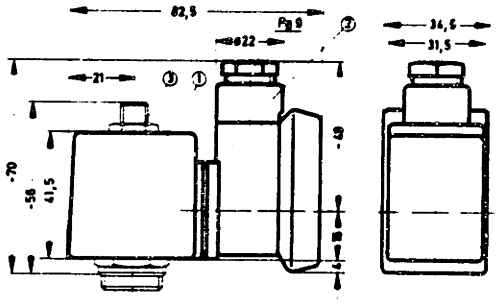

① Solenoid turns on armature tube
② Connector can be shifted 90°
③ Tightening torque of fastening nut min. 200, max. 400 Ncm

Order designation			
DC voltage		AC voltage 50 and 60 Hz	
Part No.	Type Voltage	Part No.	Type Voltage Frequency
4956	MSXG - 12	6715	MSXW - 24 - 50/60
4957	MSXG - 24	6716	MSXW - 42 - 50/60
		6717	MSXW - 110 - 50/60
		6650	MSXW - 220 - 50/60

Order designation (see table)	Type MSXG + voltage	Type MSXW + voltage
Design	DC voltage solenoid	AC voltage solenoid
Voltages Standard	12, 24 V	24, 42, 110, 220 V/50 and 60 Hz
Special	6 to 220 V	36 to 380 V/50 Hz, 48 to 240 V/60 Hz
Permissible voltage fluctuations	± 10%	± 10%
Permissible frequency fluctuations	-	± 5%
Power consumption for standard voltage*	10.3 W at 12 V 10.8 W at 24 V	50 Hz: Hold 18 VA, Pull 29 VA 60 Hz: Hold 15 VA, Pull 24 VA
Percentage duty cycle	100%	
Degree of protection as per DIN 40050	IP 65	
Threaded cable connector	Pg 9	
Ambient temperature	-5 to +60° C	
Temperature of medium	-10 to +60° C	
Min. starting time	14 ms	
Weight	0.195 kg	0.180 kg

* for special voltages on request